6.4 Examination of Development Commencing

6.4.1 General

Regarding the timing of development of this Project, the yardstick tentatively will be when the supply capability becomes less than demand.

The timing of development of this Project is assumed in this Report to be after Paute-C Power Station has started operation. INECEL has planned development of a number of sites as projects to follow commissioning of Paute-C Power Station. Consequently, it is looked forward to that the next development site will be decided upon a comprehensive study of technology, economic natures, funding plans, etc.

In this section, it is assumed that the year of development of the Chespi Project will be between 1993 and 1997, and a study is made of the demand and supply balance in the case this Project is considered.

Electric energy from hydroelectric power stations is to be applied with priority as supply capacity. Supply from thermal power plants will be made in the event a shortage in supply capacity occurs with hydroelectric power sources.

In the event a supply shortage occurs even when all hydro and thermal power stations are operated, the supply shortages are to be calculated by month. The year of development of the Chespi Project is to be estimated making judgments on the results of this study.

A flow chart on calculation of demand and supply balance is given in Fig. 6-1.

6.4.2 Considerations on Demand and Supply Balance

The balance of demand and supply for the period from 1993 to 1997 is studies to estimate the year of commissioning of Chespi Hydroelectric Power Station.

The supply facilities considered are based on data of electric power facility construction plans prepared by INECEL for the period up to 1995. That is, the power supply facilities to be developed from the present time, 1985, up to 1995 are to be used as the energy supply capability, while regarding the power supply facilities prior to 1985, the operating performance record of 1984 is used. As for hydroelectric power stations, the energy supply is computed by electric energy simulation as previously mentioned. Further, with regard to thermal power stations, the thermal power station scrapping program of INECEL is to be considered in the study of the demand and supply balance.

The electric energy from the hydroelectric facilities, existing and to be developed by 1993, totalling 1,526 MW, will be an average of 7,186 GWh for the 20-year hydrological period from 1965 to 1984, the maximum energy production being 8,860 GWh and the minimum 4,952 GWh.

By month, the energy production will be the most in July with 810 GWh. On the other hand, the minimum will be in December with 429 GWh, the ratio to maximum energy being low at 53 percent. This is thought to be due to the fact that almost all of the present hydroelectric power generating facilities being located in the Amazon River Basin and are governed by the hydrological characteristics of that basin.

The power demand and supply balances of the individual years from 1993 to 1997 are considered to be as follows:

a) Energy Balance in 1993

Of the 7,186 GWh of energy from hydroelectric power generating facilities, 6,201 GWh (86.3 percent) will be effectivized, and this effective energy will correspond to 86.5 percent of total electric energy demand.

The remaining electric energy demand of 970 GWh is to be supplied from the 699 MW of thermal facilities at that time. It will also be possible to supply from the thermal facilities during the entire period at times of lowest water (excess probability 5 percent) in individual months during the hydrological period.

b) Energy Balance in 1994

Of the electric energy of hydroelectric power stations, 6,438 GWh (89.6 percent) will be effectivized. This effective energy corresponds to 83.3 percent of total electric energy demand.

The remaining energy demand of 1,290 GWh is to be supplied by the 619 MW of thermal facilities existing in that year. However, on examining the times of lowest water in the individual months during the hydrological period, there will be shortages in supply capability in February and December. Especially, in December, even when thermal power stations are operated at high load, there will be a supply shortage of 28.5 GWh in the year of lowest water.

c) Energy Balance in 1995

Of the electric energy of hydroelectric power stations, 92.4 percent, or 6,639 GWh, will be effectivized. The effective energy will correspond to 80.1 percent of total energy demand.

Regarding the remaining energy demand of 1,654 GWh, if it is to be supplied by the 607 MW of thermal facilities existing in that year, the equipment utility factor of thermal power stations will be 31.1 percent.

However, when the times of lowest water in the individual years are examined, there will be shortages in supply occurring in January, February, November, and December. Particularly, it can be seen that a shortage of 86 GWh will be produced in December during the hydrological period.

d) Energy Balance in 1996

Of the electric energy of hydroelectric facilities, 95.6 percent, or 6,868 GWh, will be effectivized, and this corresponds to 75.1 percent of total energy demand.

The remaining energy demand, 2,280 GWh, or 24.9 percent of the total energy demand, would be supplied by the thermal power generating facilities existing in that year. The thermal power generating facilities of that year will be 581 MW, with the equipment utility factor 44.8 percent. However, in December, even when seen in terms of average value, it will become impossible for supply to be made with the installed thermal capacity of that year.

Further, in low-water years, there will be supply shortages for a half-year - January, February, March, October, November, and December. The month of the greatest shortage will be December, and there will be a supply shortage in 11 years out of the hydrological period of 20 years.

e) Energy Balance in 1997

Of the electric energy of hydroelectric power stations, 97.6 percent, or 7,011 GWh, will be effectivized, and this will correspond to 71.4 percent of total energy demand.

The remainiong energy demand of 2,809 GWh corresponds to 28.6 percent of total energy demand. This remaining energy demand is to be supplied with the thermal power stations existing in that year. The equipment utility factor of thermal power stations will be 64.8 percent. However, in the months of January, February, November, and December, when looked upon from the standpoint of average electric energy during the hydrological period, supply cannot be accomplished with thermal facilities. Further, in low-water years, there will be supply shortages in months other than June, July, and August.

The results of the above are shown in Table 6-27, 6-28, 6-29, 6-30, 6-31 and Fig. 6-3..

6.4.3 Examination Results of Development Commencing

According to the study on the demand and supply balance giving consideration to the national system, it is known that there is a great variation in monthly electric energy. The reason for this is thought to be the fact that the locations of hydroelectric power stations are one-sided. Shortages in electric energy are predominant at the beginning and end of the year. The monthly variation in electric energy will become exceptionally prominent after Paute-C Power Station has gone into operation. Therefore, in order to reduce the monthly variation in electric energy, and moreover, to supplement shortages in energy at the beginning and end of the year, it would be desirable that projects of different hydrological characteristics will be developed.

It is anticipated that a small amount of energy shortage will occur in January 1994. This shortage in electric energy will be produced in the month of lowest water during the hydrological period, but it whould be possible to overcome this shortage in energy as the quantity is small.

It is expected there will be a slightly large energy shortage at the end of 1994 and the beginning of 1995, and this trend will increase year after year. Even if thermal power stations are operated at full load, there will be a chronic shortage in energy from the end of 1996.

If this Project is to start operation in the middle part of the 1990s, it will be reasonable for the year of commissioning to be 1995. This recommendation is deduced from the study of demand and supply balance. In this case the electric energy of the Chespi Project will become potensialized for several years if the energy of existing hydroelectric power stations were to be applied to demand on a priority basis.

However, it is known that internal rate of return will not be changed greatly even if the year of start-up were to be delayed a year or two. Therefore, the year of start of operation is to be left as mentioned above to carry out financial and economic evaluations of the Project.

Needless to mention, it is looked forward to that a final decision on the year of commissioning will be made by INECEL upon consideration of other projects.

Table 6–27 kWh Balance in 1993 (Without Chespi P/S)

Item / Month		Jan.	Feb.	Mar.	Apr.	May	Jun.	Jul.	Aug.	Sep.	Oct.	Nov.	Dec.	Total
1 Energy Demand	(GWh)	603.9	577.3	606.8	594.6	613.9	586.0	585.2	596.0	576.6	609.6	598.1	624.0	7,172.0
2 Hydro Effective Energy	(GWh)	429.7	459.3	574.2	707.8	700.8	735.3	810.2	726.8	604.8	574.7	433.9	428.9	7,186.4
3 Hydro Salable Energy	(GWh)	426.6	439.7	534.7	574.9	580.0	568.6	578.7	577.2	535.0	533.4	428.2	424.2	6,201.3
4 Hydro Effective Ratio (3/2)	(%)	99.3	95.7	93.1	81.2	82.8	77.3	71.4	79.4	88.5	92.8	98.7	98.9	86.3
5 Other Necessary Energy (1 - 3)	(GWh)	177.3	137.6	72.1	19.7	33.9	17.4	6.5	18.8	41.6	76.2	169.9	199.8	970.7
6 Thermal Installed Capacity	(MW)	699.0	699.0	699.0	699.0	699.0	699.0	699.0	699.0	699.0	699.0	699.0	699.0	-
7 Thermal Plant Factor	(%)	34.1	29.3	13.9	3.9	6.5	3.5	1.2	3.6	8.3	14.7	33.8	38.4	15.8
3' Hydro Energy in Driest Year	(GWh)	250.3	217.1	290.7	431.7	381.1	468.0	454.7	357.0	379.0	289.3	234.0	223.7	3,976.6
5' Other Necessary Energy (1 - 3')	(GWh)	353.6	360.2	316.1	162.9	232.8	118.0	130.5	239.0	197.6	320.3	364.1	400.3	3,195.4
7' Thermal Plant Factor	(%)	68.0	76.7	60.8	32.4	44.8	23.4	25.1	46.0	39.3	61.1	72.3	77.0	52.2
8 95% Thermal Effective Energy ⑥×(day)×24×0.95×0.96	(GWh)	474.3	428.4	474.3	459.0	474.3	459.0	474.3	474.3	459.0	474.3	459.0	474.3	5,584.4
9 Insufficient Energy 9 = 1 - 3' - 8	(GWh)	0	0	0	0	0	0	0	0	0	0	0	0	0
10 Insufficient Frequency in 20 Years		0/20	0/20	0/20	0/20	0/20	0/20	0/20	0/20	0/20	0/20	0/20	0/20	0/240

Table 6–28 KWh Balance in 1994 (Without Chespi P/S)

Item / Month		Jan.	Feb.	Mar.	Apr.	May	Jun.	Jul.	Aug.	Sep.	Oct.	Nov.	Dec.	Total
1 Energy Demand	(GWh)	650.6	622.0	653.7	640.6	661.3	631.3	630.5	642.1	621.3	657.0	644.4	672.2	7,727.0
2 Hydro Effective Energy	(GWh)	429.7	459.3	574.2	707.8	700.8	735.3	810.2	726.8	604.8	574.7	433.9	428.9	7,186.4
3 Hydro Salable Energy	(GWh)	429.7	447.8	545.4	605.0	607.5	602.6	621.7	613.6	558.2	548.2	431.2	426.6	6,437.7
4 Hydro Effective Ratio (3 / 2)	(%)	100.0	97.5	95.0	85.5	86.7	82.0	76.7	84.4	92.3	95.4	99.4	99.5	89.6
5 Other Necessary Energy (1 - 3)	(GWh)	220.9	174.2	108.3	35.6	53.8	28.7	8.8	28.5	63.1	108.8	213.2	245.6	1,289.5
6 Thermal Installed Capacity	(MW)	619.0	619.0	619.0	619.0	619.0	619.0	619.0	619.0	619.0	619.0	619.0	619.0	-
7 Thermal Plant Factor	(%)	48.0	41.9	23.5	8.0	11.7	6.4	1.9	6.2	14.2	23.6	47.8	53.3	23.8
3' Hydro Energy in Driest Year	(GWh)	250.3	217.1	407.3	431.7	381.1	468.0	454.7	357.0	379.0	289.3	234.0	223.7	4,093.2
5' Other Necessary Energy (1 - 3')	(GWh)	400.3	404.9	246.4	208.9	280.2	163.3	175.8	285.1	242.3	367.7	410.4	448.5	3,633.8
7' Thermal Plant Factor	(%)	86.9	97.3	53.5	46.9	60.8	36.6	38.2	61.9	54.4	79.8	92.1	97.4	67.0
8 95% Thermal Effective Energy ⑥×(day)×24×0.95×0.96	(GWh)	420.0	379.4	420.0	406.5	420.0	406.5	420.0	420.0	406.5	420.0	406.5	420.0	4,945.3
9 Insufficient Energy 9 = 1 - 3' - 8	(GWh)	0	25.5	0	0	0	0	0	0	0	0	3.9	28.5	57.9
10 Insufficient Frequency in 20 Years		0/20	1/20	0/20	0/20	0/20	0/20	0/20	0/20	0/20	0/20	1/20	1/20	3/240

Table 6–29 KWh Balance in 1995 (Without Chespi P/S)

Item / Month	Jan.	Feb.	Mar.	Apr.	May	Jun.	Jul.	Aug.	Sep.	Oct.	Nov.	Dec.	Total
1 Energy Demand (GWh)	698.3	667.6	701.6	687.5	709.9	677.5	676.7	689.1	666.8	704.9	691.6	721.5	8,293.0
2 Hydro Average Energy (GWh)	429.7	459.3	574.2	707.8	700.8	735.3	810.2	726.8	604.8	574.7	433.9	428.9	7,186.4
3 Hydro Effective Energy (GWh)	429.7	451.5	555.0	633.8	633.5	634.9	660.7	641.8	577.6	557.9	433.6	428.9	6,638.9
4 Hydro Effective Ratio (3／2) (%)	100.0	98.3	96.7	89.5	90.4	86.3	81.5	88.3	95.5	97.1	99.9	100.0	92.4
5 Other Necessary Energy(1－3) (GWh)	268.6	216.1	146.6	53.7	76.4	42.6	16.0	47.3	89.2	147.0	258.0	292.6	1,654.1
6 Thermal Installed Capacity (MW)	607.0	607.0	607.0	607.0	607.0	607.0	607.0	607.0	607.0	607.0	607.0	607.0	-
7 Thermal Plant Factor (%)	59.5	53.0	32.5	12.3	16.9	9.7	3.5	10.5	20.4	32.6	59.0	64.8	31.1
3' Hydro Energy in Driest Year (GWh)	250.3	217.1	290.7	431.7	381.1	468.0	454.7	357.0	379.0	289.3	234.0	223.7	3,976.6
5' Other Necessary Energy(1－3') (GWh)	448.0	450.5	410.9	255.8	328.8	209.5	222.0	332.1	287.8	415.6	457.6	497.8	4,316.4
7' Thermal Plant Factor (%)	99.2	110.4	91.0	58.5	72.8	47.9	49.2	73.5	65.9	92.0	104.7	110.2	81.2
8 95% Thermal Effective Energy (GWh)	411.9	372.0	411.9	398.6	411.6	398.6	411.6	411.6	398.6	411.6	398.6	411.9	4,849.3
9 Insufficient Energy 9 = 1 - 3' - 8 (GWh)	36.1	78.5	0	0	0	0	0	0	0	4.0	59.0	85.9	263.5
10 Insufficient Frequency in 20 Years	3/20	3/20	0/20	0/20	0/20	0/20	0/20	0/20	0/20	1/20	2/20	2/20	11/240

Table 6-30 KWh Balance in 1996 (Without Chespi P/S)

Item / Month		Jan.	Feb.	Mar.	Apr.	May	Jun.	Jul.	Aug.	Sep.	Oct.	Nov.	Dec.	Total
1 Energy Demand	(GWh)	770.3	736.4	773.9	758.4	783.0	747.4	746.5	760.2	735.5	777.6	762.9	795.9	9,148.0
2 Hydro Average Energy	(GWh)	429.7	459.3	574.2	707.8	700.8	735.3	810.2	726.8	604.8	574.7	433.9	428.9	7,186.4
3 Hydro Effective Energy	(GWh)	429.7	455.0	565.4	668.1	666.6	672.1	712.7	673.9	594.8	566.9	433.9	428.9	6,868.0
4 Hydro Effective Ratio (3/2)	(%)	100.0	99.1	98.5	94.4	95.1	91.4	88.0	92.7	98.3	98.6	100.0	100.0	95.6
5 Other Necessary Energy(1 - 3)	(GWh)	340.6	281.4	208.5	90.3	116.4	75.3	33.8	86.3	140.7	210.7	329.0	367.0	2,280.0
6 Thermal Installed Capacity	(MW)	581.0	581.0	581.0	581.0	581.0	581.0	581.0	581.0	581.0	581.0	581.0	581.0	-
7 Thermal Plant Factor	(%)	78.8	72.1	48.2	21.6	26.9	18.0	7.8	20.0	33.6	48.7	78.7	84.9	44.8
3' Hydro Energy in Driest Year	(GWh)	250.3	217.1	290.7	431.7	381.1	468.0	454.7	357.0	379.0	289.3	234.0	223.7	3,976.6
5' Other Necessary Energy(1 - 3')	(GWh)	520.0	519.3	483.2	326.7	401.9	297.4	291.8	403.2	356.5	488.3	528.9	572.2	5,171.4
7' Thermal Plant Factor	(%)	-	-	-	-	-	-	-	-	-	-	-	-	-
8 95% Thermal Effective Energy	(GWh)	394.2	356.0	394.2	381.5	394.2	381.5	394.2	394.2	381.5	394.2	381.5	394.2	4,641.4
9 Insufficient Energy 9 = 1 - 3' - 8	(GWh)	125.8	163.3	89.0	0	7.7	0	0	9.0	0	94.1	147.4	178.0	814.3
10 Insufficient Frequency in 20 Years		10/20	6/20	1/20	0/20	0/20	0/20	0/20	1/20	0/20	3/20	8/20	11/20	40/240

Table 6–31 KWh Balance in 1997 (Without Chespi P/S)

Item \ Month		Jan.	Feb.	Mar.	Apr.	May.	Jun.	Jul.	Aug.	Sep.	Oct.	Nov.	Dec.	Total
1 Energy Demand	(GWh)	826.8	790.5	830.8	814.1	840.6	802.3	801.3	816.0	789.5	834.7	819.0	854.4	9,820.0
2 Hydro Average Energy	(GWh)	429.7	459.3	574.2	707.8	700.8	735.3	810.2	726.8	604.8	574.7	433.9	428.9	7,186.4
3 Hydro Effective Energy	(GWh)	429.7	457.7	571.1	684.3	684.5	698.6	750.6	697.0	602.3	572.6	433.9	428.9	7,011.2
4 Hydro Effective Ratio (3／2)	(%)	100.0	99.7	99.5	96.8	97.7	95.0	92.6	95.9	99.6	99.6	100.0	100.0	97.6
5 Other Necessary Energy(1－3)	(GWh)	397.1	332.8	259.7	129.8	156.1	103.7	50.7	119.0	187.2	262.1	385.1	425.5	2,808.8
6 Thermal Installed Capacity	(MW)	469.0	469.0	469.0	469.0	469.0	469.0	469.0	469.0	469.0	469.0	469.0	469.0	-
7 Thermal Plant Factor	(%)	113.8	105.6	74.4	38.4	44.7	30.7	14.5	34.1	55.4	75.1	114.0	122.0	68.4
3' Hydro Energy in Driest Year	(GWh)	250.3	217.1	290.7	431.7	381.1	468.0	454.7	357.0	379.0	289.3	234.0	223.7	3,976.6
5' Other Necessary Energy(1－3')	(GWh)	576.5	573.4	540.1	382.4	459.5	334.3	346.6	459.0	410.5	545.4	585.0	630.7	5,843.4
7' Thermal Plant Factor	(%)	-	-	-	-	-	-	-	-	-	-	-	-	-
8 95% Thermal Effective Energy	(GWh)	318.2	287.4	318.2	308.0	318.2	308.0	318.2	318.2	308.0	318.2	308.0	318.2	3,746.8
9 Insufficient Energy 9 = 1 - 3' - 8	(GWh)	258.3	286.0	221.9	74.4	141.3	26.3	28.4	140.8	102.5	227.2	277.0	312.5	2,096.6
10 Insufficient Frequency in 20 Years		13/20	12/20	7/20	2/20	3/20	2/20	1/20	2/20	3/20	6/20	14/20	15/20	80/240

Fig. 6–3 Energy Demand (Without Project)

(Total Demand from Hydro Effective Energy)

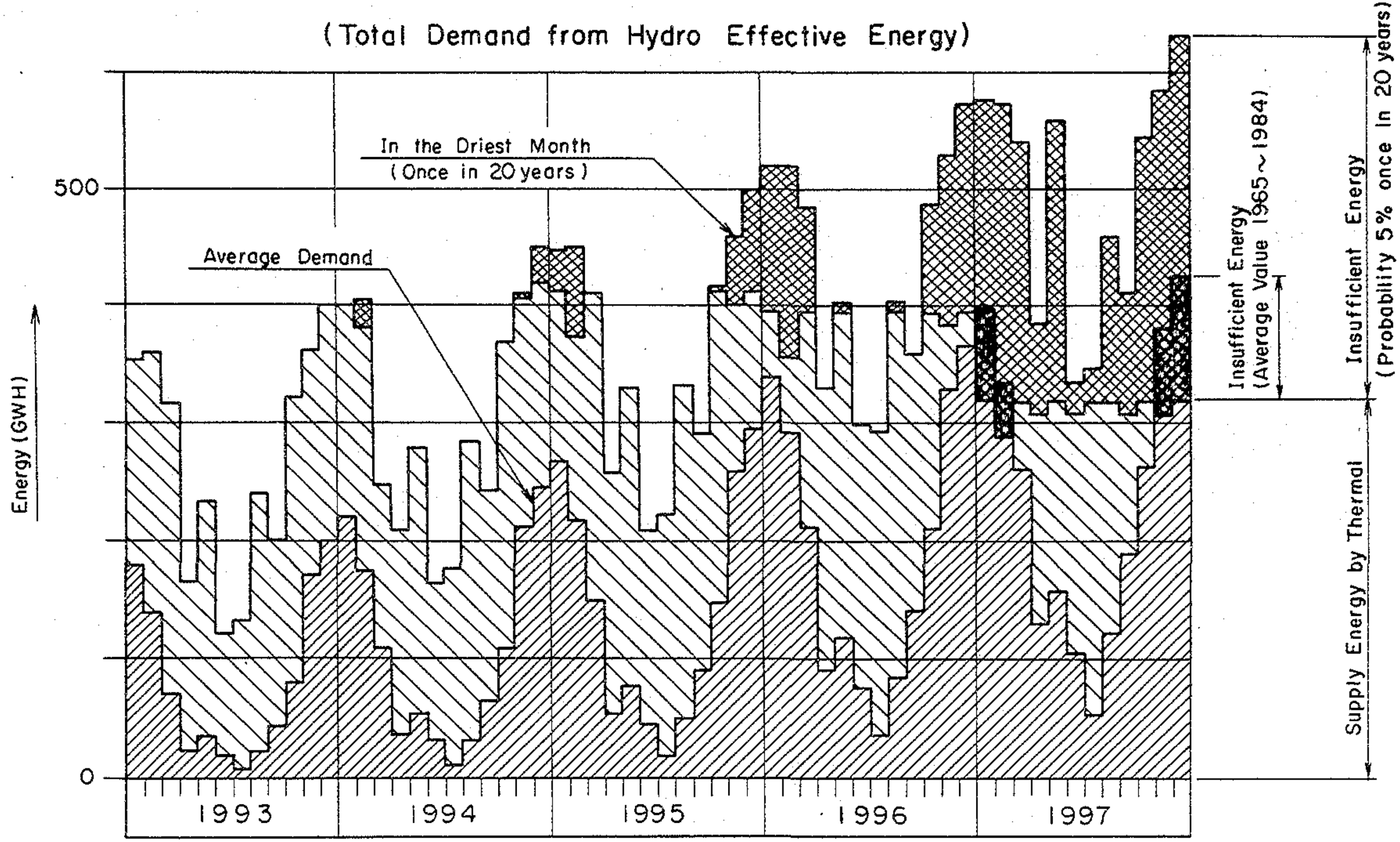

CHAPTER 7 PRELIMINARY DESIGN

CHAPTER 7 PRELIMINARY DESIGN

CONTENTS

TABLE LIST

FIGURE LIST

DRAWING LIST

CHAPTER 7 PRELIMINARY DESIGN

7.1 Dam

7.1.1 Selection of Dam Site

The topographical and geological factors from the standpoint of dam structure in the vicinity of the dam axis decided on at the master plan level were considered, as for the special characteristic of this site, which is sedimentation, and a dam site where flushing could be most effectively performed was selected. This dam site, including the reservoir, is a location which is optimum from a structural standpoint as described in geology. Topgraphically, both banks are steeply sloped, and an ideal layout can be made for structures such as the spillway, flushing facilities, intake, etc.

As for sedimentation and flushing of sediment, it will be possible to discharge sediment collected in the reservoir by flushing once yearly in a year of average inflow and about thrice yearly in a high-water year as described in 7.1.2, and it will be possible to maintain the functions of the dam by doing so.

7.1.2 Sedimentation in Reservoir and Flushing

1) General

Studies are made of the mode of sedimentatiion in the resrvoir and the mode of sediment discharge by flushing constituting the most important problem for Chespi Power Station. Simulation of the sedimentation will start from January 1, since it is not definite yet when the power station is to be commissioned. The wash-out gate is to be opened and flushing done when the reservoir has become full of sediment with the gate closed when the sediment trapped has been completely discharged downstream and water storage is again started. Power generation without impairing the functions of the dam will be made possible throught repetitions of the above operations.

2) Basic Equation

a) Continuous Equations of Sediment

The river-bed variation is handled as the average cross-sectional quantity, and is to be expressed by the equations below:

$$\Delta Z = \frac{Q'B - QB}{B\Delta x\ (1 - \lambda)} \Delta t \quad \ldots\ldots (1)$$

$$\Delta Z = Z_{(t + 1)} - Z_t \quad \ldots\ldots (2)$$

where,

ΔZ : river-bed variation within time t

$Q'B$: sediment inflow from upstream cross section

Qb : sediment outflow from downstream cross section

B : river-bed variation range

λ : void ratio (= 0.4)

Z : river-bed height

ΔX : distance of section

b) Suspended Load Equation

In river-bed variations, suspended load is the governing factor according to the results of various tests on field materials and relevant data of INECEL, and calculations using suspended load were carried out.

Lane-Kalinske's Equation

$$q_s = q \cdot C_o\ P/\sigma \quad \ldots\ldots\ldots\ldots\ldots\ldots\ldots\ldots (3)$$

$$C_o = 5.55 \Delta F(w_o)\ [1/2(\frac{u*}{wo})\ \exp\ - (\frac{wo}{u*})^{2}\ ]^{1.61} \quad (4)$$

where,

qs: suspended load per unit width and unit time

q: runoff per unit width

P: function of K, V, U* according to the figure below

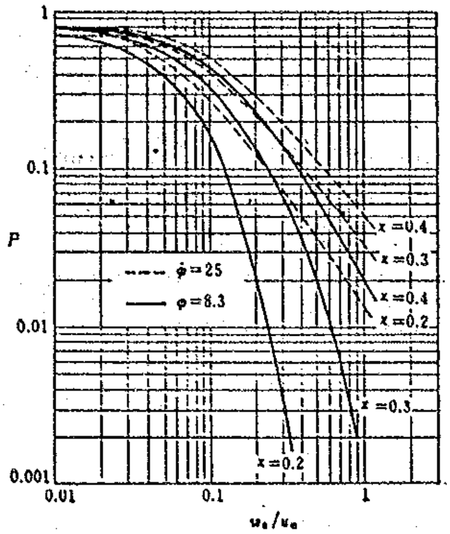

Note) For Karman's constant K, 0.4 is used

Co : river-bed concentration (ppm)

$\Delta F(w_0)$: proportion of sand particles of settling velocity (w_0) in river-bed sand gravel (%)

σ : unit weight of sediment particles

c) Settling Velocity (w_0)

This is calculated by the equations below.

$$d(\text{cm}) \geqq 0.58 : w_0 = 73.2d^{1/2}$$

$$0.58 > d \geqq 0.11: \quad Wo = 81.5d^{0.667}$$

$$0.11 > d \geqq 0.015: Wo = 171.5d$$

$$0.015 > d: Wo = 11940.0d^2$$

d) Total Sediment Inflow

$$Q_B = q_s \times B \times 10^{-4} /(1 - \lambda)$$

3) Calculation Sequence

The procedure of calculations is as follows:

(1) Nonuniform flow calculations are performed for runoff at time to for the initial river-bed condition.

(2) Friction velocity (u*) is determined for each cross section.

(3) The Quantity of load is determined for each particle size by the load quantity equation.

(4) Q_B is determined by the total sum of the above load quantities.

(5) The river-bed variation quantity is obtained by (1), and the river-bed height after variation is obtained from (2).

(6) Calculations according to the above (1) to (5) are repeated until the required sedimentation for the reservoir is obtained.

(7) When the reservoir has become filled with sediment, the wash-out gate is opened to make an open channel, the same calculations as described above are made, and the sediment accumulated in the reservoir is removed.

(8) When discharge of sediment from the reservoir has been completed, the wash-out gate is closed and the calculations from (1) above are restarted using the cross-sectional area after accomplishment of sediment discharge.

4) Calculation Conditions

a) Grain-Size Distribution and Properties of Reservoir Sediment

a)-1 Grain-Size Distribution Curve

On measuring the grain-size distributions of the present river-bed materials deposited at the dam site with the purpose of estimating the variation in river-bed configuration inside the dam reservoir, the grain-size distribution curves shown in Fig. 7.1 are obrained.

Fig. 7-1 Grain-Size Distribution Curve

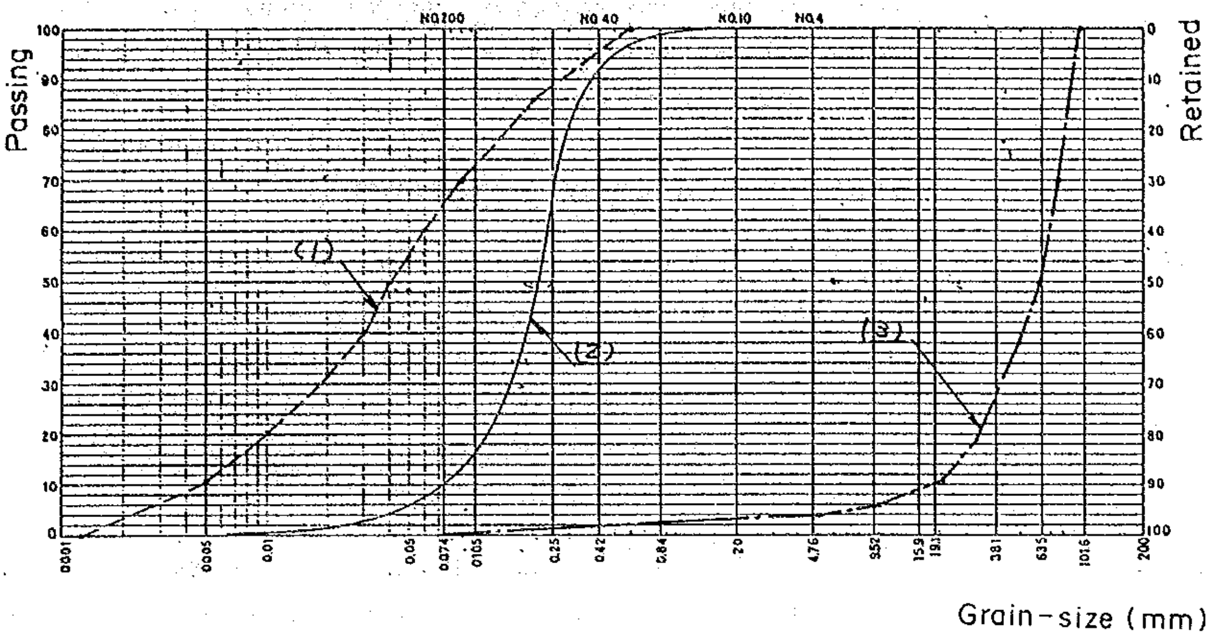

Eq. (1): A.J. Cubi Gaging Station average suspended load

Eq. (2): Chespi dam site sampled sediment

Eq. (3): A.J. Cubi Gaging Station average river-bed sediment

There are the grain-size distribution equations (1) to (3) above, and Eq. (2) will be used here in view of the difference between grain-size distributions during flood and during low water.

The reason is that Eq. (2) is for actual sedimentation at a dam site, and because the difference between Eqs. (1) and (3) is large and the calculations will become very complex unless a single grain-size distribution curve is used for sediment flowing in daily. Therefore, Eq. (2), close to the average of the whole is employed.

In accordance with the abové, the values shown in Table 7-1 are used as grain-size distribution in Eq. (2) for sedimentation calculations.

The sediment inflow is divided into the two groups, that is, suspended material and bed load. The above mentioned two quantities are changeable depending on the inflow discharge into the regulating pondage, accordingly the calculation combined with the Curve (1) and the Curve (3) is very complicated.

On the other hand, it is quite important subject in the Feasibility Study whether the function of regulating pondage is secured, and that the number of times of flushing out a year is checked if the flushing out is possible so that the more detailed study has to be performed at the stage of definite study.

The grain-size of sediment material in the Curve (1) is very fine and the size less than 0.1 mm contains about 70%, therefore the affect to turbine is judged to be small. And the quantity of the Curve (3) is estimtaed to be about 10% of the total sediment quantity. Accordingly, the Curve (2), which is analyzed the sedimented material at the damsite where the run-off velocity being low, is established and used for this study to make simplify the calculation.

Table 7–1 Grain-size Distribution

Representative Diometer (mm)	1.1	0.54	0.37	0.23	0.14	0.09	0.04
Percentage (%)	2	5	11	48	17	8	9

a)-2 Component Analysis of Inflowing Stream Water

The result of component analysis on stream water is as shown in Table 7-2. Since the table gives the values of just one analysis, they are to be used only as references. As may be seen in the table, there is no factor to be of a special problem in the water of the Rio Guayllabamba.

Table 7-2 The Results of Component Analysis of Rio Guayllabamba

	P.H	Suspension material (mg/l)	Si (mg/l)	Al (mg/l)	Fe (mg/l)	Ca (mg/l)	Mg (mg/l)	Na (mg/l)	K (mg/l)	Cl (mg/l)	So_4 (mg/l)
Chespi	7.90	93	21.6	ND	ND	22.3	22.9	46.1	7.3	31.1	23.4
Detectable Limit			6.2	0.62	0.11	0.32	0.026	0.053	0.060	1.8	4.1

Note 1) Water fifltered with millipore filter (0.45μ) used except for suspended solids (SS).

2) Cl was obtained by the test for chloride content of marine sand (Japan Society of Civil Engineers, Japan Road Association), SO_4 by the weight analysis method using barium sulfate, and the others by the atomic absorption analysis method.

3) ND indicates "less than detection limit."

4) Sample water was collected at A.J. Cubi Gaging Station on January 21, 1985.

a)-3 Component Analysis of Inflow Sediment

The components of sediment flowing into the reservoir were analyzed by X-ray examinations. The results are given in Fig. 7-2 and Table 7-3. Enlarged photomicrographs of the individual components are shown from the following page. The results of X-ray analysis show that 50 percent of the sediment flowing in is plagioclase. The materials are mostly fresh and it is thought there is a large quantity of relatively hard minerals of Mohs hardness 5 and higher.

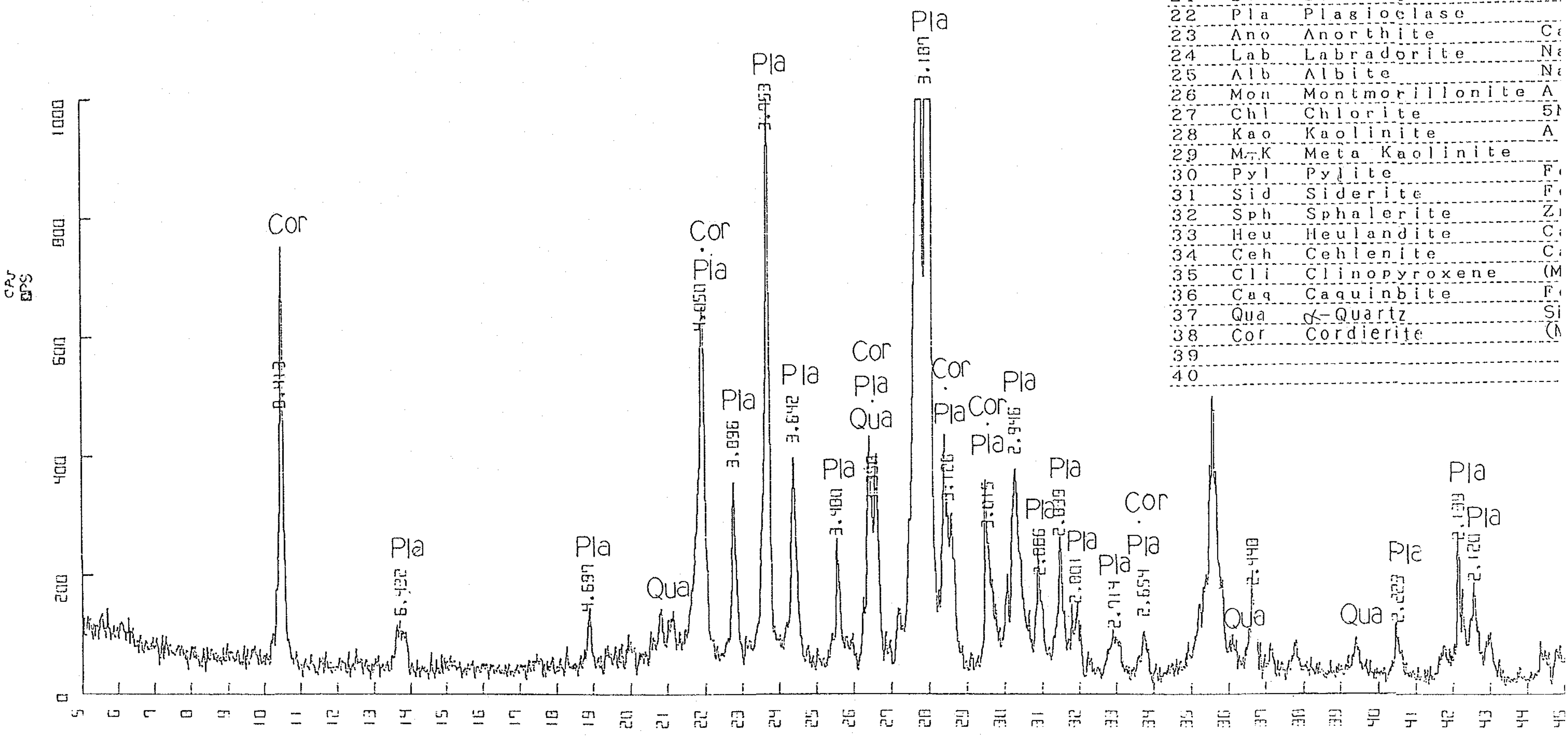

21	Ett	Ettringite	C
22	Pla	Plagioclase	
23	Ano	Anorthite	C
24	Lab	Labradorite	N
25	Alb	Albite	N
26	Mon	Montmorillonite	A
27	Chl	Chlorite	5
28	Kao	Kaolinite	A
29	M-K	Meta Kaolinite	
30	Pyl	Pylite	F
31	Sid	Siderite	F
32	Sph	Sphalerite	Z
33	Heu	Heulandite	C
34	Ceh	Cehlenite	C
35	Cli	Clinopyroxene	(M
36	Caq	Caquinbite	F
37	Qua	α-Quartz	Si
38	Cor	Cordierite	(M
39			
40			

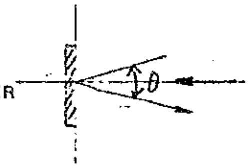

21	Ett	Ettringite	$Ca_6Al_2(SO_4)_3(OH)_{12}\cdot 25H_2O$
22	Pla	Plagioclase	
23	Ano	Anorthite	$CaAl_2Si_2O_8$
24	Lab	Labradorite	$NaAlSi_3O_8\cdot CaAlSi_2O_8$
25	Alb	Albite	$NaAlSi_3O_8$
26	Mon	Montmorillonite	$Al_2O_3\cdot 4SiO_2\cdot 6H_2O$
27	Chl	Chlorite	$5Mgo\cdot Al_2O_3\cdot 3SiO_2\cdot 4H_2O$
28	Kao	Kaolinite	$Al_2Si_2O_5(OH)_4$
29	M-K	Meta Kaolinite	
30	Pyl	Pylite	FeS_2
31	Sid	Siderite	$FeCO_3$
32	Sph	Sphalerite	ZnS
33	Heu	Heulandite	$CaAl_2Si_7O_{18}\cdot 6H_2O$
34	Ceh	Cehlenite	$Ca_2Al_2Si_1O_7$
35	Cli	Clinopyroxene	$(Mg,Fe)SiO_3$
36	Caq	Caquinbite	$Fe_2(SO_4)_3\cdot 9H_2O$
37	Qua	α-Quartz	SiO_2
38	Cor	Cordierite	$(Mg,Fe)_2Al_4Si_5O_{18}$
39			
40			

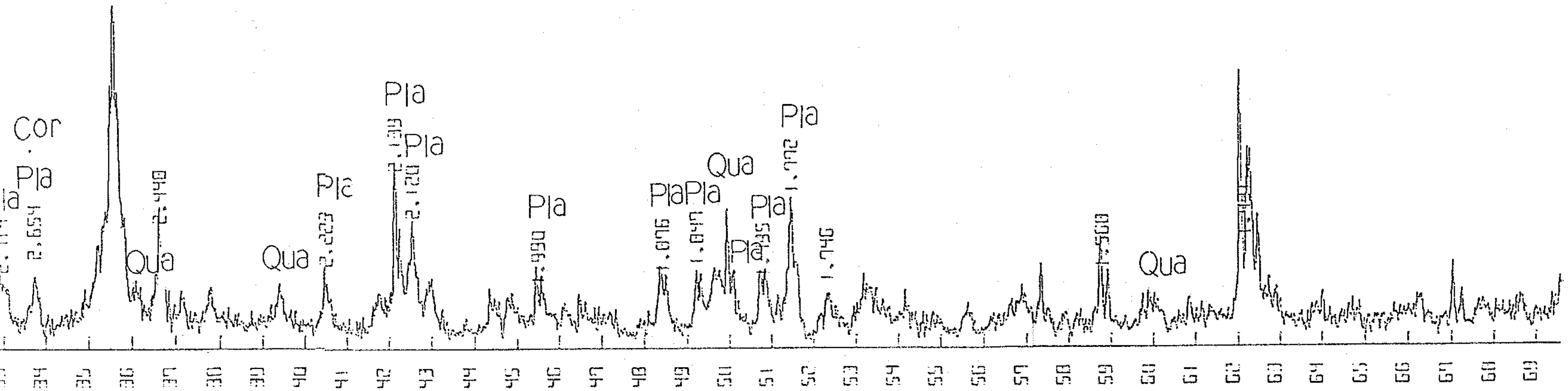

ANGLE	INTEN	D-VALUE	FWHM
10.499	406	8.413	0.300
13.751	72	6.432	0.300
18.880	80	4.697	0.360
21.918	520	4.050	0.300
22.793	293	3.896	0.300
23.680	863	3.753	0.300
24.417	330	3.642	0.300
25.576	196	3.480	0.300
26.522	251	3.358	0.320
27.974	2204	3.187	0.320
28.531	222	3.126	0.200
29.596	213	3.015	0.280
30.311	340	2.946	0.340
30.952	127	2.886	0.240
31.482	168	2.839	0.260
31.917	71	2.801	0.160
32.965	55	2.714	0.320
33.740	78	2.654	0.280
35.625	441	2.518	0.360
36.675	110	2.448	0.280
40.540	70	2.223	0.280
42.206	208	2.139	0.220
42.610	131	2.120	0.220
45.540	44	1.990	0.280
48.462	65	1.876	0.280
49.276	73	1.847	0.280
50.826	49	1.795	0.280
51.532	169	1.772	0.300
52.340	54	1.746	0.340
58.834	68	1.568	0.280
62.161	99	1.491	0.140

ANGLE	INTEN	D-VALUE	FWHM
10.499	465	8.413	0.300
13.751	116	6.432	0.300
18.880	124	4.697	0.300
21.918	535	4.050	0.300
22.793	366	3.896	0.300
23.680	932	3.753	0.300
24.417	407	3.642	0.300
25.576	250	3.480	0.300

GEIGERFLEX RAD :
TARGET/FILTER(MONOCHRO) :
VOLTAGE/CURRENT : 40 KV/ 30 MA
STEP WIDTH : 0.02DEG
PRESET TIME : 0.4SEC
ANGLE ZOOM : 2
SMOOTHING : 3

Table 7–3 Microscopic Observation

Sample No. CHESPI Date Apr,1985

Thin-Section No, A-1 Observed by K,Iguchi

Texture ; River sand (unconsolidated) . Sample obtained by quartering, and microscope specimencs were made on embedding in resin.

Description

Hardness (Mohs)	Mineral	Vol.%	Feature
6	Plagioclase	50	Coloress,prominent zoning , strong automorphic nature, mostly comparativerly fresh.
6	Hornblende	15	Green or brown with pleohroism. Strong auttmorphic nature, mostly comparatively fresh.
5 ~6	Augite	5	Strong automorphic nature. Light brown.
6	Opaque Minerals	5	Mostly strongly magnetic and assumed to be magnetite. The four minerals hereinabove mostly in form of individual sand particles.
	Rock fragment		
?	(Basalt)	10	Andesitic basalt. Roughly the same as andesite below.
?	(Andesite)	10	Plagioclase and hornblende are observed as phenocrysts. Hornblende altered in parts.
3	(Limestone)	≒0	Rock fragments of calcite or rock altered and metasomatized into calcite recognized.
?	(Mudstone)	≒0	Fragments of argillaceous rock are observed.
7	Quartz	≒0	Fractically no individual sand particle seen, but exists together with plagioclase in fine granophyre.

Note ; Vol % roughly reckoned by visual observation.

Others ; Almost grains range in diameter from 0.1 to 0.6 mm and are not rounded. Although eliminated in making thin section, roud gravels of about φ 5 mm were also contained.

Comment ; Comparatively hard minerals of Mohs hardness 5 or over make up at least 80 percent of whole.

x 50

x 100

x 200

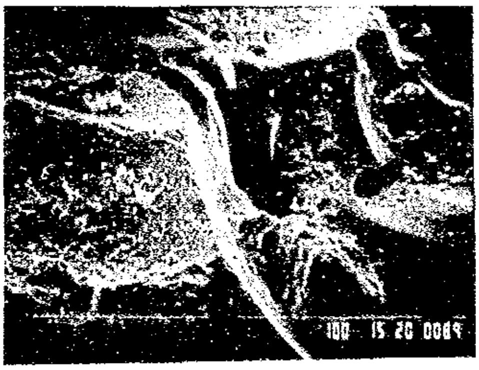

x 500

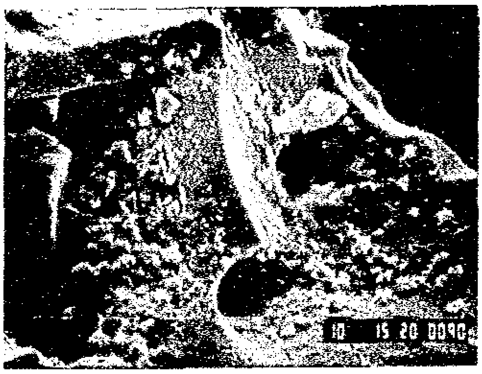

x 1000

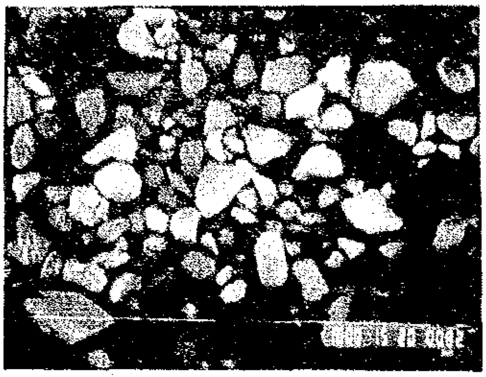

x 50

x 100

x 200

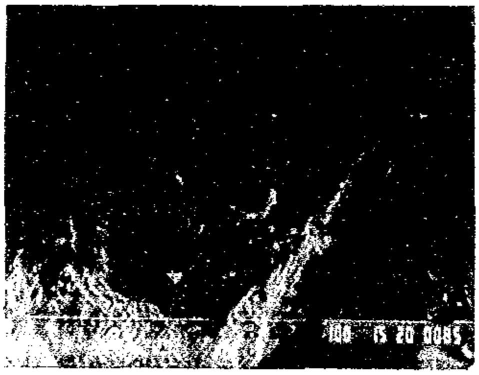

x 500

x 50

x 100

x 200

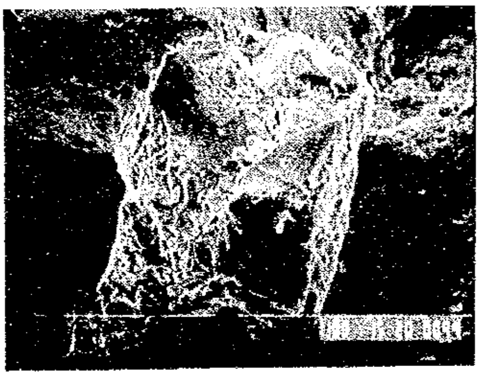

x 500

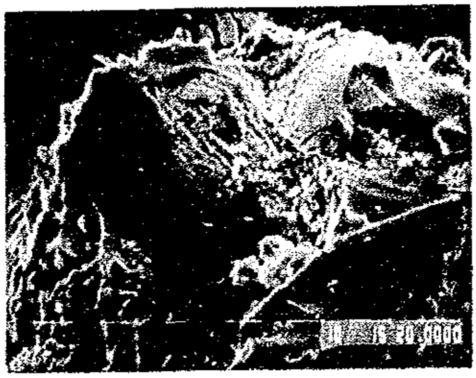

x 1000

x 50

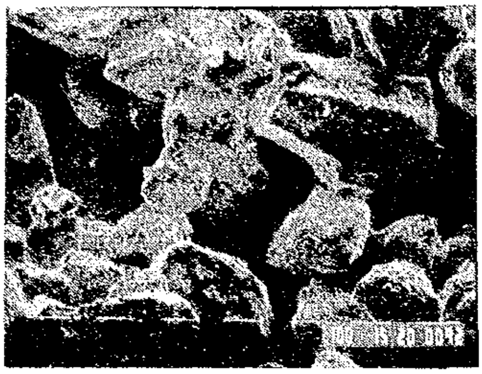

x 100

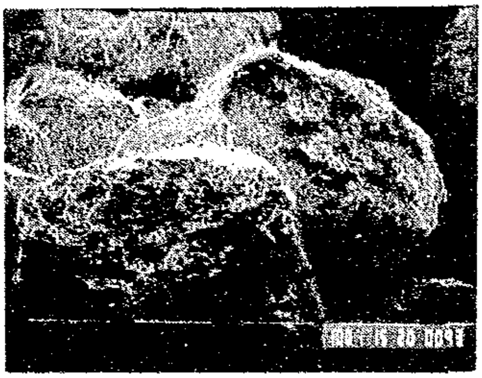

x 200

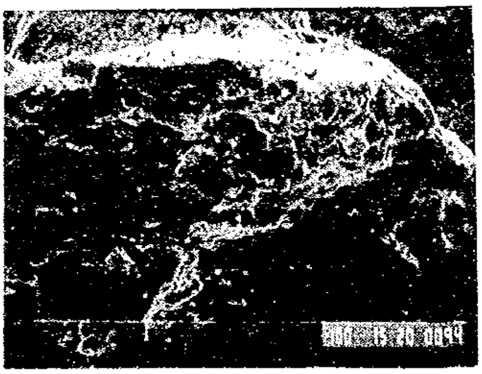

x 500

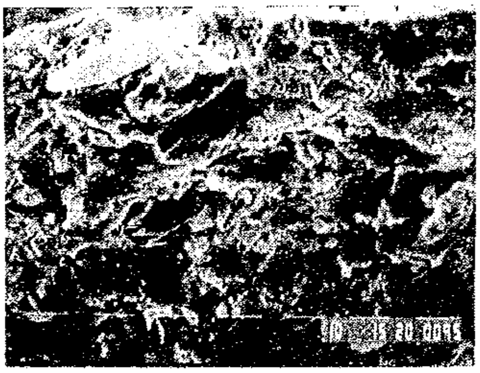

x 1000

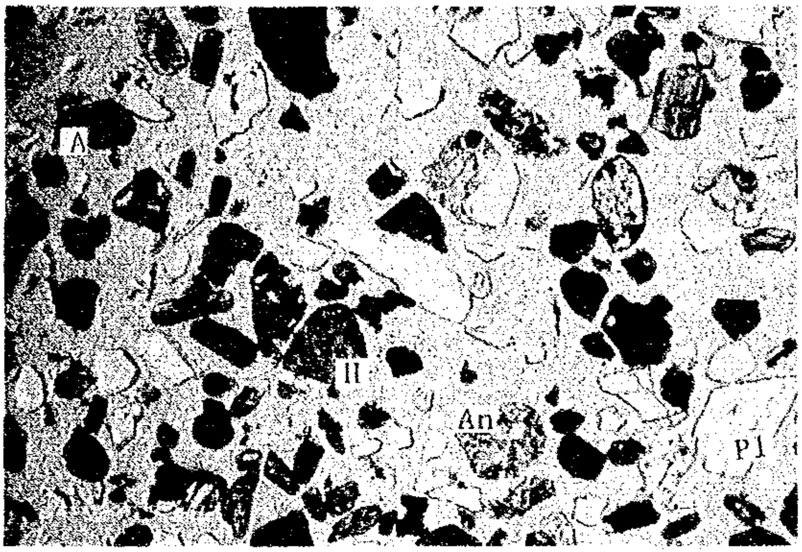

open 4 x 10

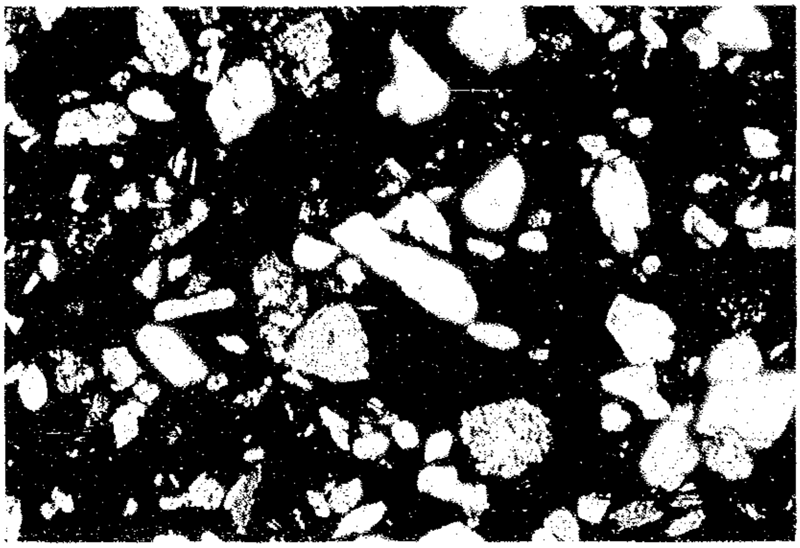

close 4 x 10

LEGEND

Pl	Plagioclase
H	Hornblende
A	Augite
Op	Opaque minerals
Ba	Fragment of Basalt
An	Fragment of Andesite
Md	Fragment of Mudstone
Q	Quartz

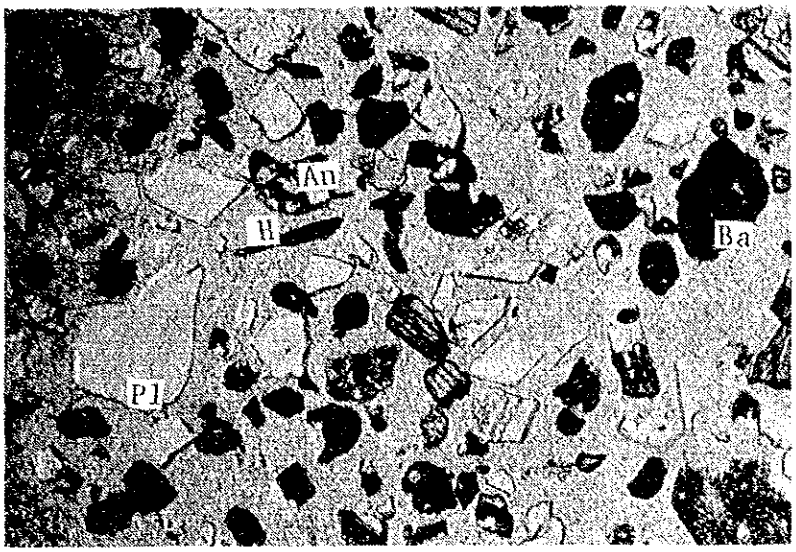

open 4 x 10

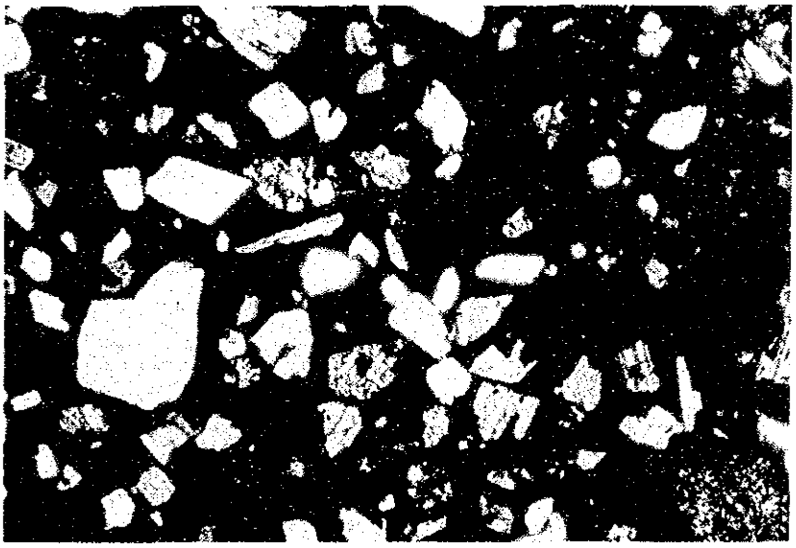

close 4 x 10·

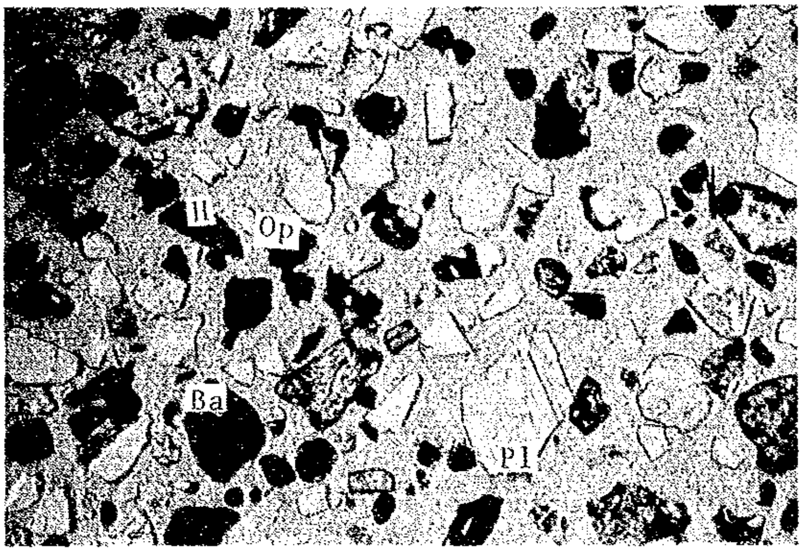

open 4 x 10

close 4 x 10

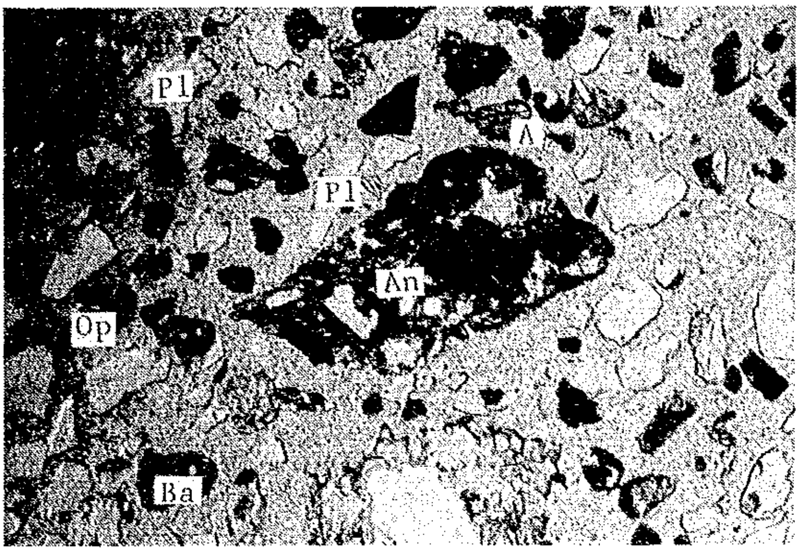

0 1mm open 4 x 10

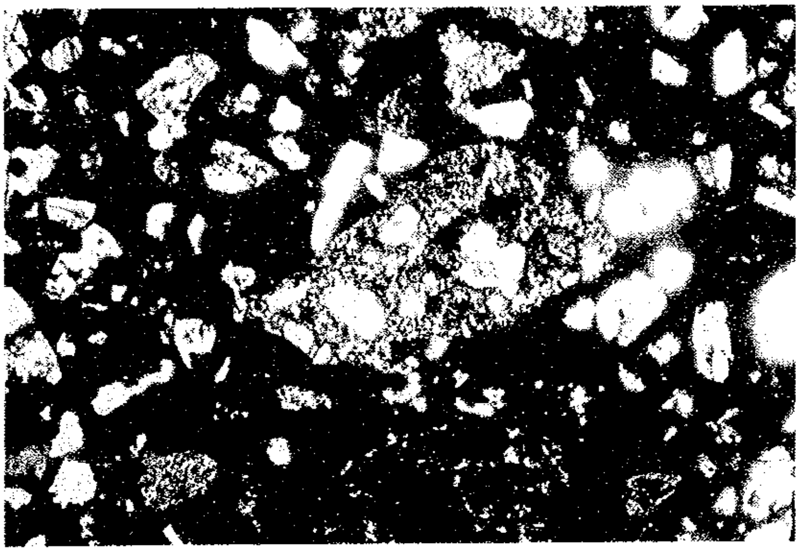

0 1mm close 4 x 10

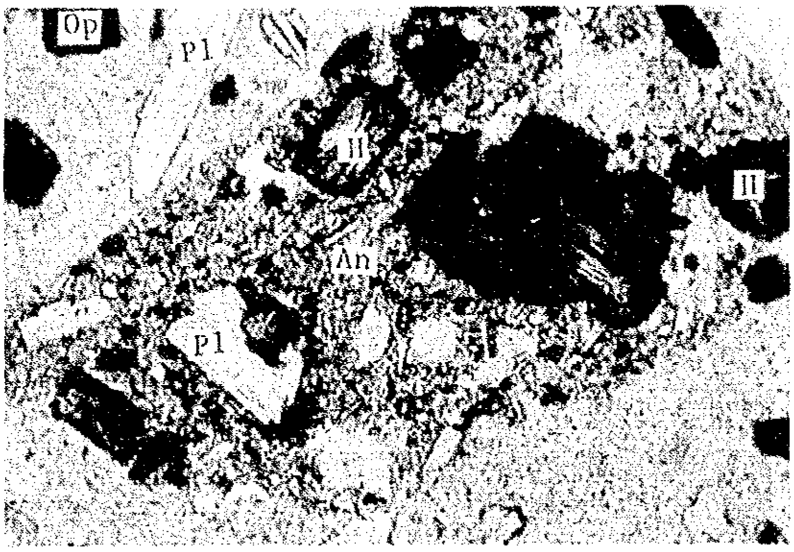

open 10 x 10

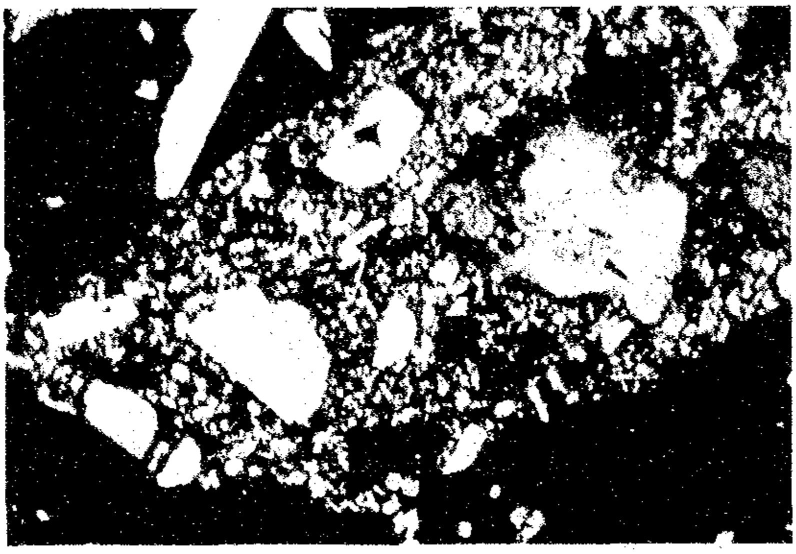

close 10 x 10

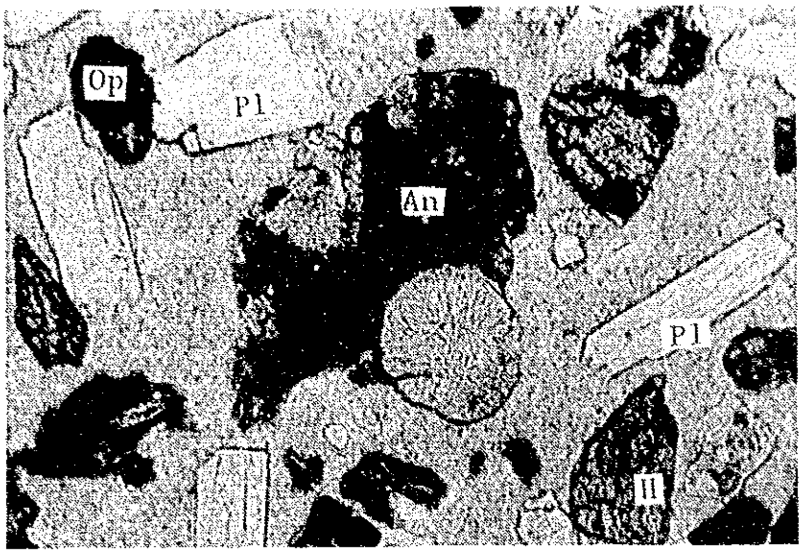

open 10 x 10

close 10 x 10

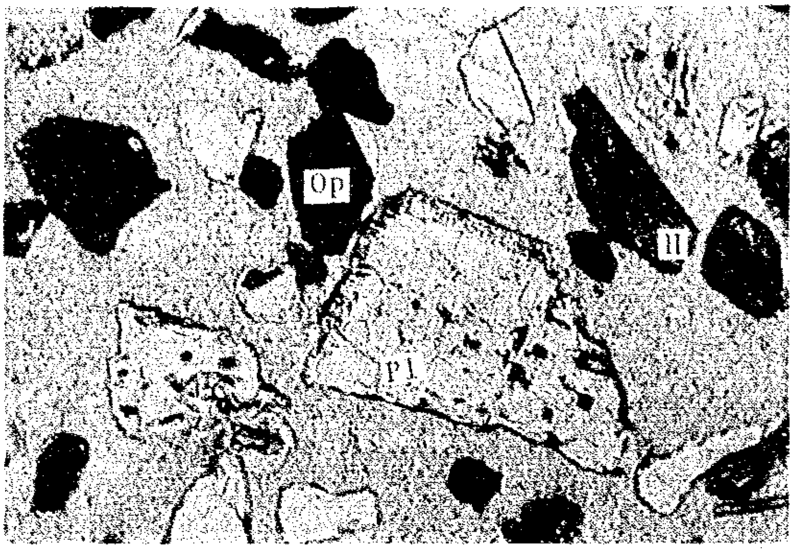

open 10 x 10

close 10 x 10

b) Years Calculated

According to the data obtained from INECEL the estimation formula for sediment inflow quantity is

$$\text{Log } Q = 0.337 \text{ Log } Qs + 1.156$$

from which

$$Qs = 0.03197 \times Q^{2.967}$$

where,

Qs: sediment inflow quantity (ton/day)

Q: A.J. Cubi Gaging Station runoff (m^3/s)

The annual inflow quantities determined using the above are given in Table 7-4.

Table 7-4 The Annual Sediment Inflow Quantities of Chespi Dam

($x10^3$ ton)

1965	1966	1967	1968	1969	1970	1971	1972
3450	1393	1639	1772	2914	6938	5380	6017
1973	1974	1975	1976	1977	1978	1979	1980
-	-	-	4486	-	938	598	1498
1981	1982	Average					
982	2858	2915					

From these results, 1972 (wet year), 1978 (dry year), and 1982 (average-water year) are selected as representative years, and calculations are made assuming that the respective inflows will continue for 3 years.

c) Runoff Data

For dam inflow data, the respective data of A.J. Cubi Gaing Station for wet year, low-water year, and average-water year are converted for the dam site by means of the following equation.

$$Q = 1.19 \times Qc$$

where,

Q: inflow at dam site (m^3/s)

Qc: inflow at A.J. Cubi Gaging Station

d) Dam Operation (Downstream End Boundary Condition)

(i) The dam water level will vary daily from high water level to low water level so that it is assumed to be constant at EL. 1,442.00 m, a median water level.

(ii) At the dam site, the wash-out gate is to be opened with EL. 1,410.00 m, which is near the median elevation of the wash-out gate, as the limit for the sedimentation level.

(iii) Sand flushing is to be considered as completed when flushing has been done to around the elevation of 1,407.50 m at the wash-out gate, at which time the gate is to be closed.

e) Results of Calculations

The results of calculations are given in Figs. 7-2 to 7-6, while the reservoir sedimentation and flushing patterns for high-water year, average-water year, and low-water year are shown in Table 7-5.

Table 7–5 The Results of Calculation in Reservoir of Chespi

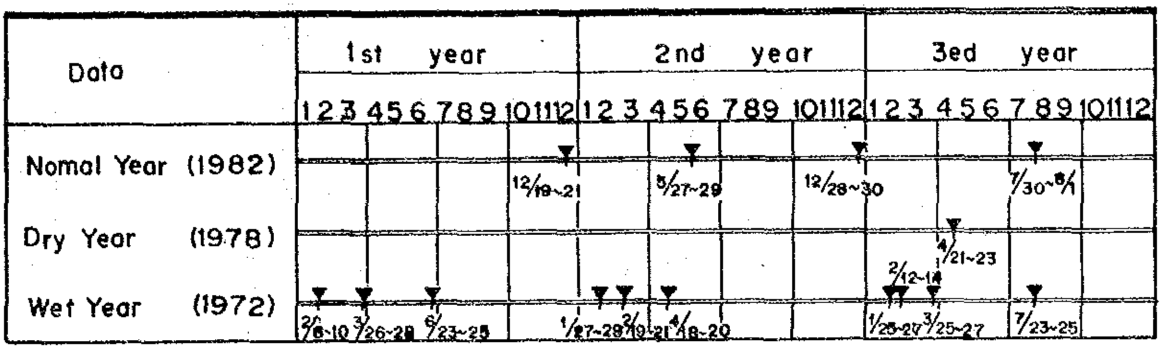

- ▼ Flushing operation
- Impoundment starts all from January 1
- Data for each year used three times repetitively

According to the above results, sediment deposited in the reservoir would be flushed three or four times a year in high-water years, once a year in average-water years, and one in 3 years in low-water years. As for the time required for a single flushing it would be approximately 6 hours for lowering the reservoir water level, approximately 48 hours for flushing, and approximately 10 hours for again storing water, a total of approximately 64 hours (approximately 3 days).

It was learned in this study that it could make clear to be possible to flush out the sediment material in the regulating pondage through the sand flush gate. It is looked forward to that more detailed sediment measurements such as correlation between run-off discharge and sediment quantity, and the grain size distribution will be carried out hereafter for the preparation of the Definite Study.

However, compounding the above mentioned Curve (1) and Curve (3) the detailed calculation has to be executed at the stage of definite study and the model test is recommended to be performed to check up the result of calculation.

Fig. 7–2 Reservoir Sedimentation Profile (Normal Year–No.1)

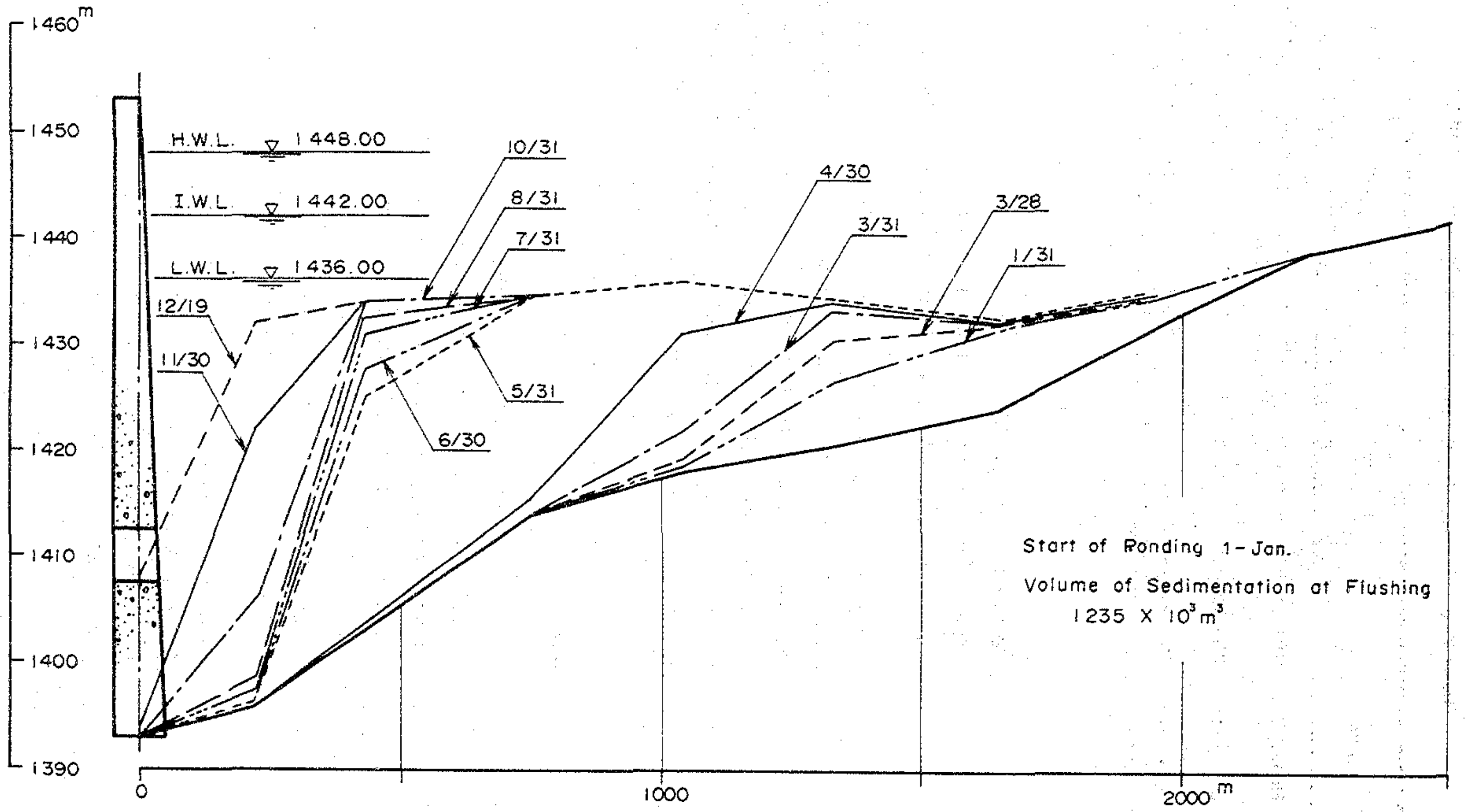

Fig. 7–3 Reservoir Sedimentation Profile (Normal Year–No.2)

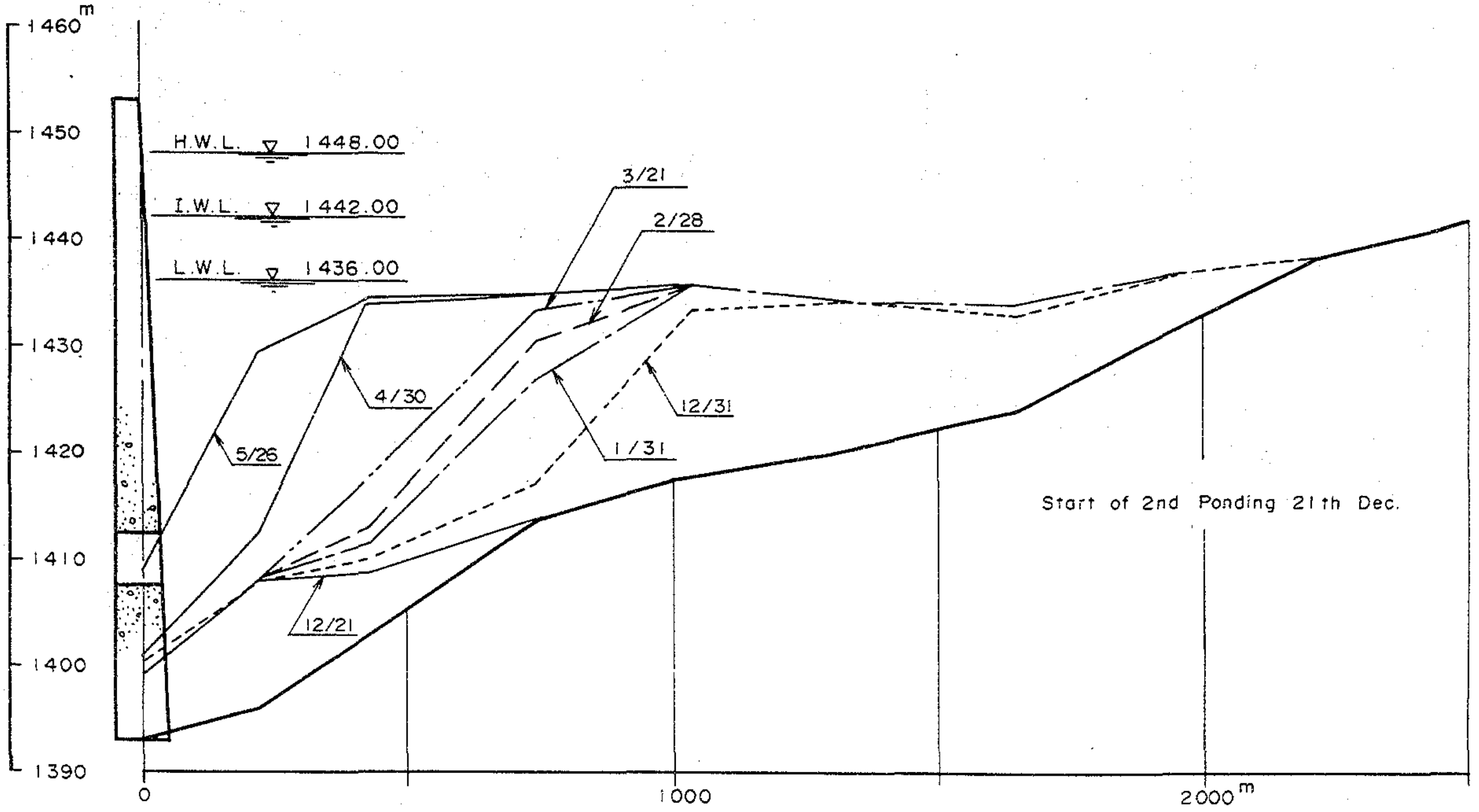

Fig. 7–4 Reservoir Sedimentation Profile (Dry Year)

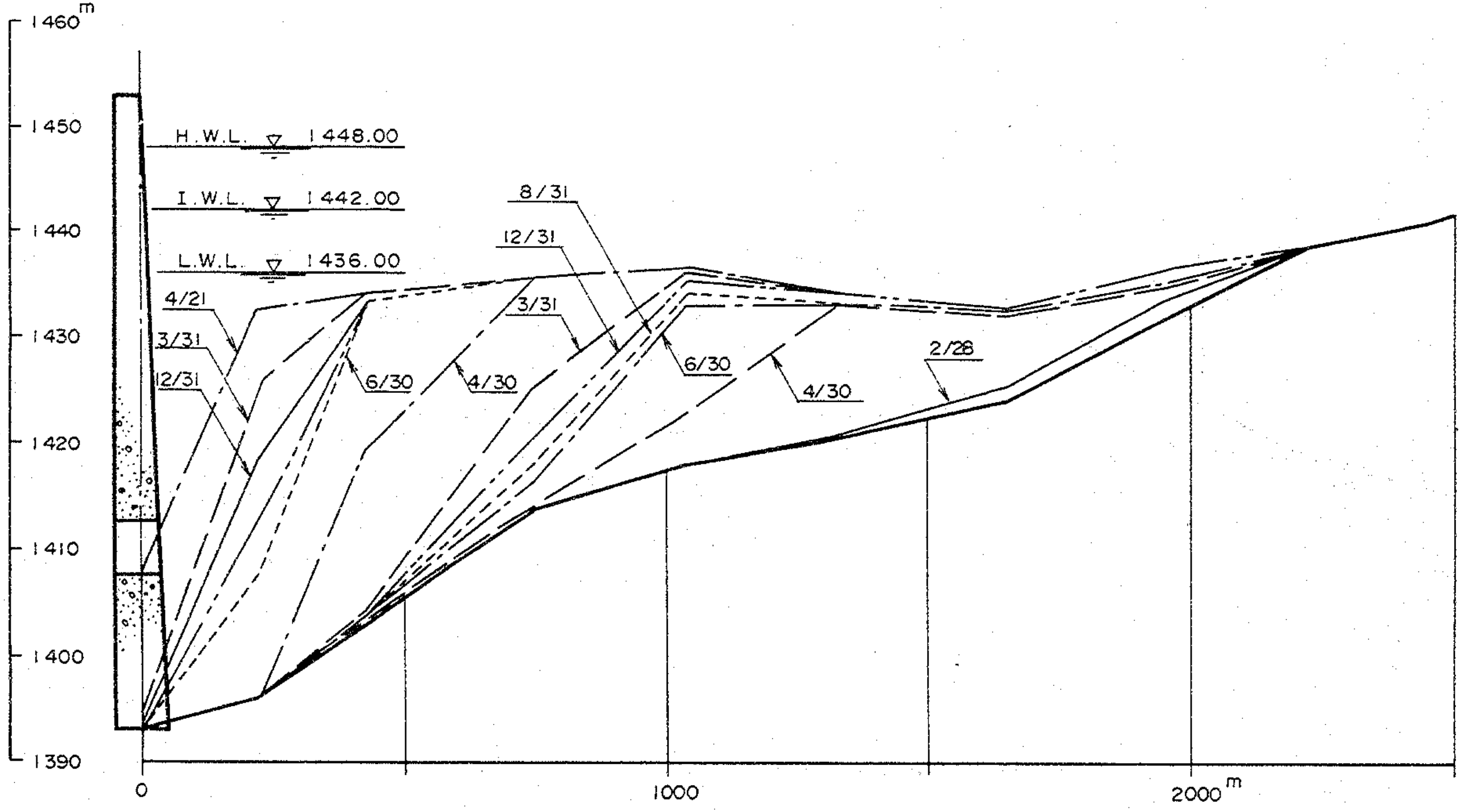

Fig. 7–5 Reservoir Sedimentation Profile (Wet Year)

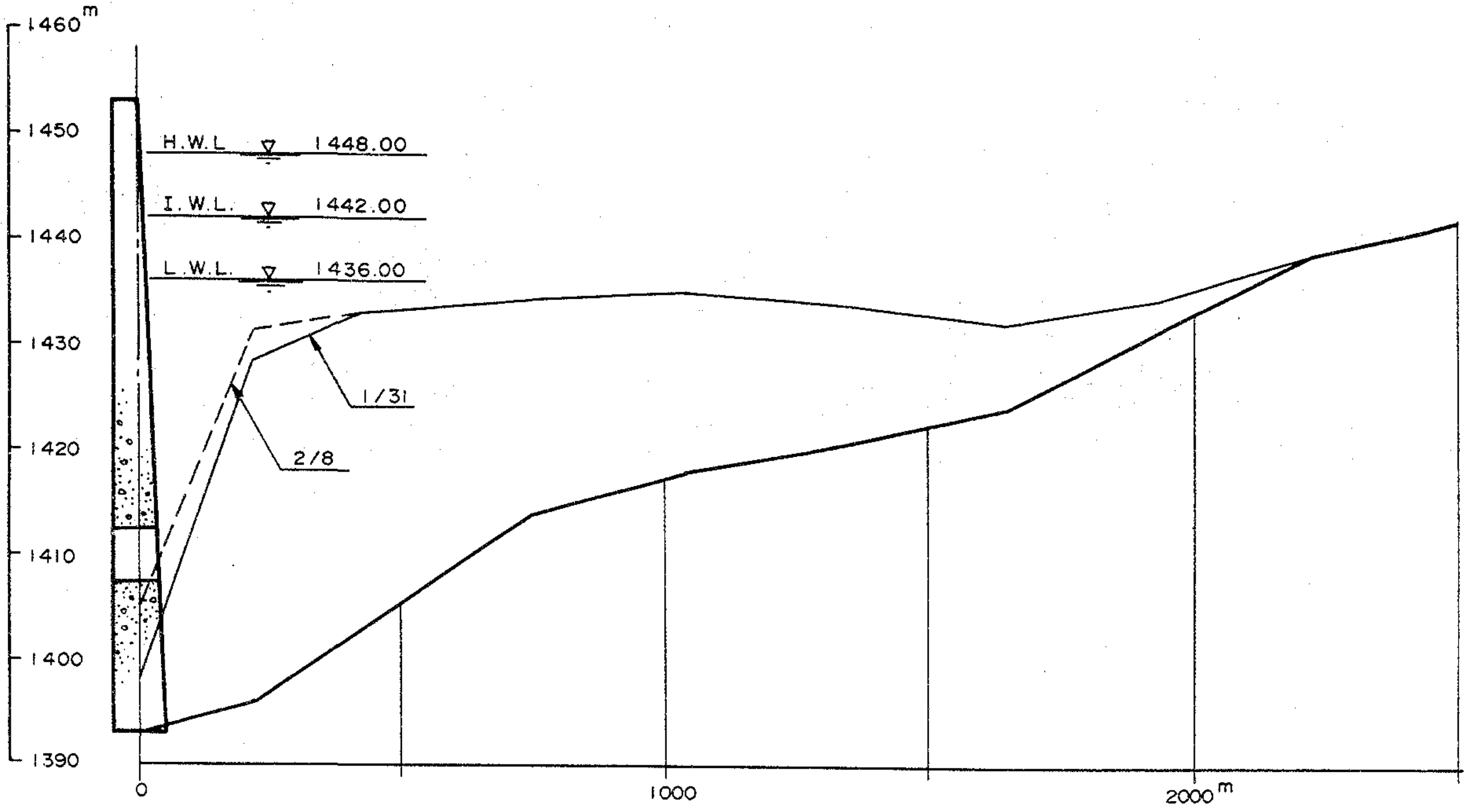

Fig. 7–6 Reservoir Flushing Profile (Normal Year)

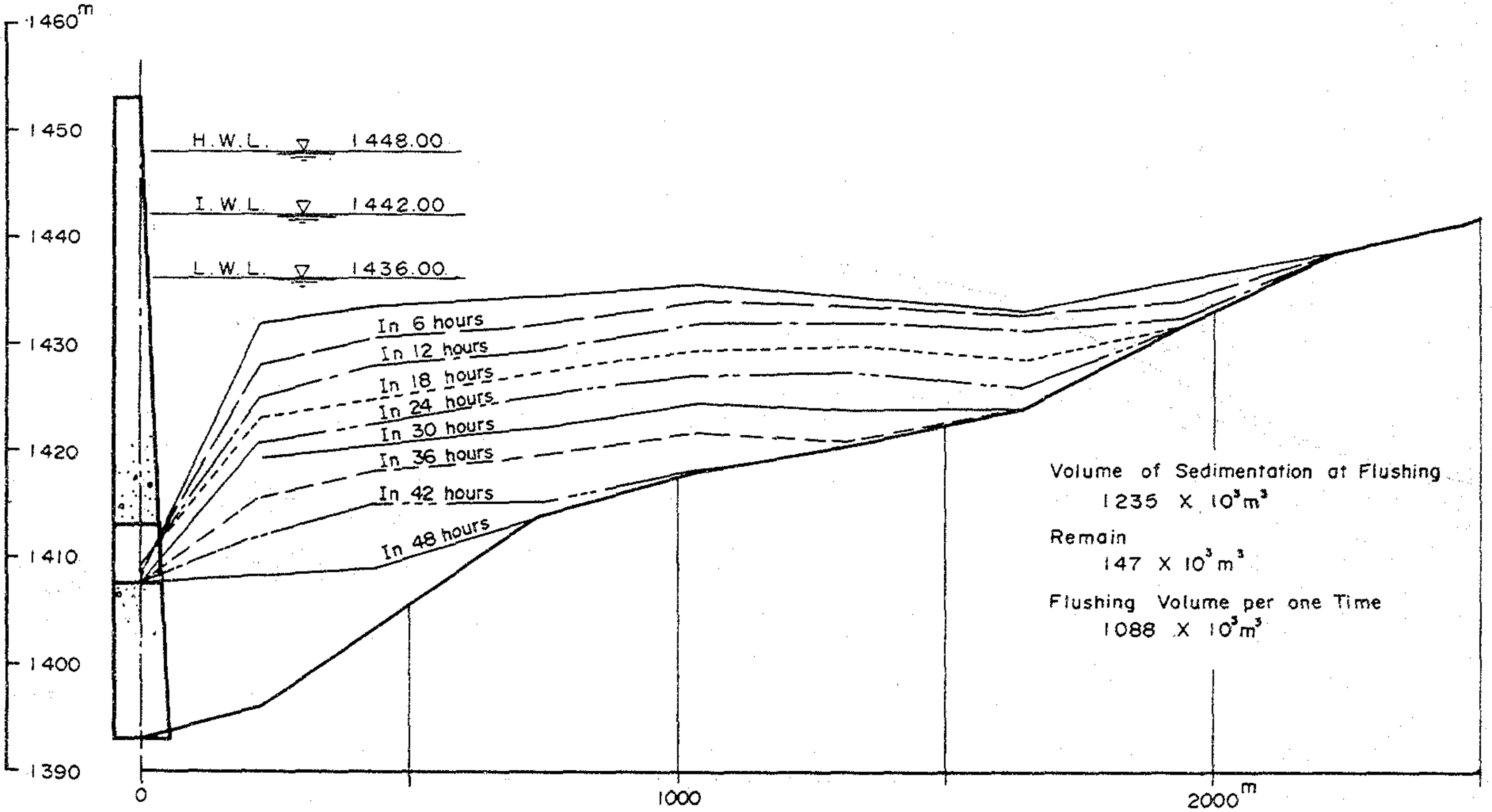

Volume of Sedimentation at Flushing
1235 X $10^3 m^3$
Remain
147 X $10^3 m^3$
Flushing Volume per one Time
1088 X $10^3 m^3$

7.1.3 Selection of Dam Type

Gravity, arch, and rockfill are conceivable as the type of the dam, but a gravity dam was selected for the Chespi site for the reason below.

(1) The topography is one in which slopes are very steep

(2) It is necessary for sand flushing facilities to be provided in the dam body.

(3) It will be possible to save on civil works costs and thus be more economical to provide the intake in the dam body rather than at the right bank.

(4) If a rockfill dam were to be selected it would be necessary to provide spillway facilities separately and when the topographical conditions are considered, that will not be economical.

7.1.4 Facilities of Dam

1) Spillway

The flood discharge applicable to the spillway is to be Q = 2,300 m^3/s according to Hydrology of which value is corresponded to 10% more than calculated 1000 years return period flood discharge.

There are a normal-use spillway and emergency-use spillway. The normal-use spillway is to be of natural overflow type with gate operation eliminated, and is to be capable of coping with flood occurring once or twice a year. The emergency-use spillway is to be of a structure that, together with the normal-use spillway, will be capable of handling past maximum flood discharge.

As for design flood discharge, it is to be possible to handle it adding the capacity of the sand flush gates.

The flood discharges handled by the individual spillways are shown in Table 7-6 and Fig. 7-7.

Table 7–6 Flood Discharge of Chespi Dam

W.L (m)	Discharge (m³/sec)				Note
	Free flow	Gate flow	Sand flash gate (x2)	Total	
1 407.5			0	0	
1 408.2			11.6	11.6	
1 409.0			32.8	32.8	
1 410.4			92.9	92.9	
1 411.9			170.6	170.6	
1 413.3			262.7	262.7	
1 414.8			367.1	367.1	
			~	~	Change flow
1 418			712.2	712.2	
1 420			798.8	798.8	
1 425			982.4	982.4	
1 430			1 136.8	1 136.8	
1 440			1 395.4	1 395.4	
1 443		0	1 464.0	1 464.0	
1 445		20.4	1 508.0	1 528.4	
1 448	0	85.2	1 571.8	1 657.0	
1 449	36.5	113.3	1 592.5	1 742.3	
1 450	109.2	144.1	1 612.8	1 866.1	
1 451	210.5	177.1	1 633.0	2 020.6	
1 452	337.3	212.1	1 653.0	2 202.4	
1 452.5	409.3	230.1	1 662.8	2 302.2	
1 453.0	487.2	248.6	1 672.6	2 408.4	

Fig. 7–7 Discharge Capacity of Spillway

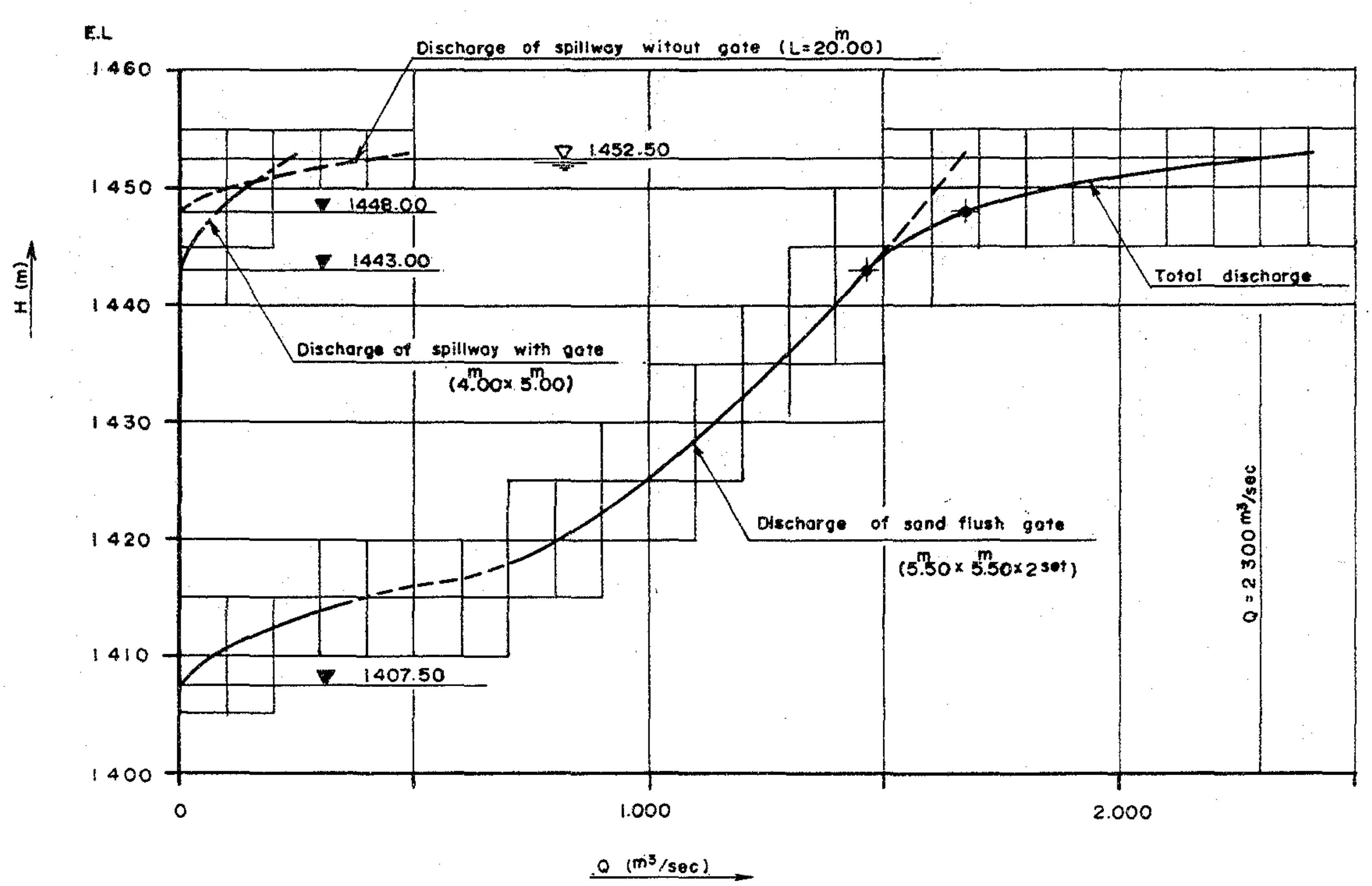

2) Height of Non-overflow Portion of Dam

In this study, the criteria of Japan and the United States of America were adopted for the calculation of clearance height.

The height of the non-overflow portion of the dam is to be obtained by the equations below.

Design water level at normal high water level:

$$h_f = h_w + h_e + h_a$$

Design water level at design flood level:

$$h_f = h_w$$

The larger of the above calculated values is to be adopted, where,

hf: added amount of required value

he: wave height due to earthquake (m)

hw: wave height due to wind (m)

ha: added value according to whether or not spillway exists (=0.5 m)

a) Wave Height Due to Earthquake

$$h_e = 1/2 \frac{k\tau}{\pi} \sqrt{gh_o}$$

where,

k: horizontal seismic coefficient (= 0.12)

τ: earthquake period (= 1.0 sec)

h_o: reservoir water depth from normal high water level (= 56.00 m)

$$h_e = 1/2 \times \frac{0.12 \times 1.0}{\pi} \times \sqrt{9.8 \times 56.00} = 0.45 \text{ m}$$

b) Wave height due to Wind

$H_w = 0.00086\ V^{1.1}\ F^{0.45}$

where,

F: fetch (= 300 m)

V: average wind speed for 10 minutes (= 30 m/s)

$h_m = 0.00086 \times 30^{1.1} \times 300^{0.45} = 0.47$ m

c) Height of Non-overflow Section

Case of design water level being normal high water level:

$h_f = h_w + h_e + h_a$

$= 0.47 + 0.45 + 0.50 = 1.42$ m

Non-overflow section elevation

1448.00 + 1.42 = 1449.50 m

Case of design flood level being flood water level

$h_f = h_w$

$= 0.47$

Non-overflow section elevation

1452.50 + 0.47 = 1453.00 m

The crest elevation of the dam was studied by two methods and the higher crest elevation was adopted. Based on high water level (HWL) + wave height by wind (hw), the crest elevation was decided.

Therefore, the height of the non-overflow section is to be 1453.00 m.

3) Diversion Scheme

There is a necessity for the stream of the Rio Guayllabamba to be diverted. The method in case the river width is broad would be multiple-stage diversion. In case the river width is narrow, there would be the method of providing a diversion tunnel and diverting the river flow at the dam site to perform work.

In this case the river width at the dam site is extremely narrow, and the best method would be for care of river to be done with a diversion tunnel.

The design flood discharge is to be the 3-year return period flood of 450 m^3/s since this is to be a concrete dam. Consequently, the tunnel diameter to discharge this flow would be 6.0 m, and the upstream cofferdam height is to be EL. 1418.00 m.

7.2 Intake

7.2.1 Type Selection

The type of the intake is determined by the sediment inflow of the Rio Guayllabamba and the grainsize distribution of the sediment. In case there is little sediment there would be no problem with an ordinary type intake as show in Fig. 7-8 where a full-face screen is provided in front of the dam or in the reservoir, but at the Chespi site, as described in 7-1. Sedimentation in Reservoir and Flushing, a surface intake-type is to be selected for reasons such as that the sediment inflow is large and grain sizes are extremely fine.

This surface intake type has the following advantages:

(i) The surface layer water of the reservoir H = 3.0 m is to be drawn so that even though sediment may arrive close to the intake immediately upstream of the dam, only the finest particles that are suspended will flow in.

(ii) Since there is peripheral concrete protecting the cylinder gate at the front of the intake, even if the sediment surface in the reservoir were to rise higher than planned it would not be an obstacle to power generation.

(iii) Since the cylinder gate rises and falls in accordance with the fluctuation in the reservoir water level, by installing a screen at the upper part of the cylinder gate it will not be necessary for a screen to be stretched over the entire surface.

Fig. 7-8 Type of Intake

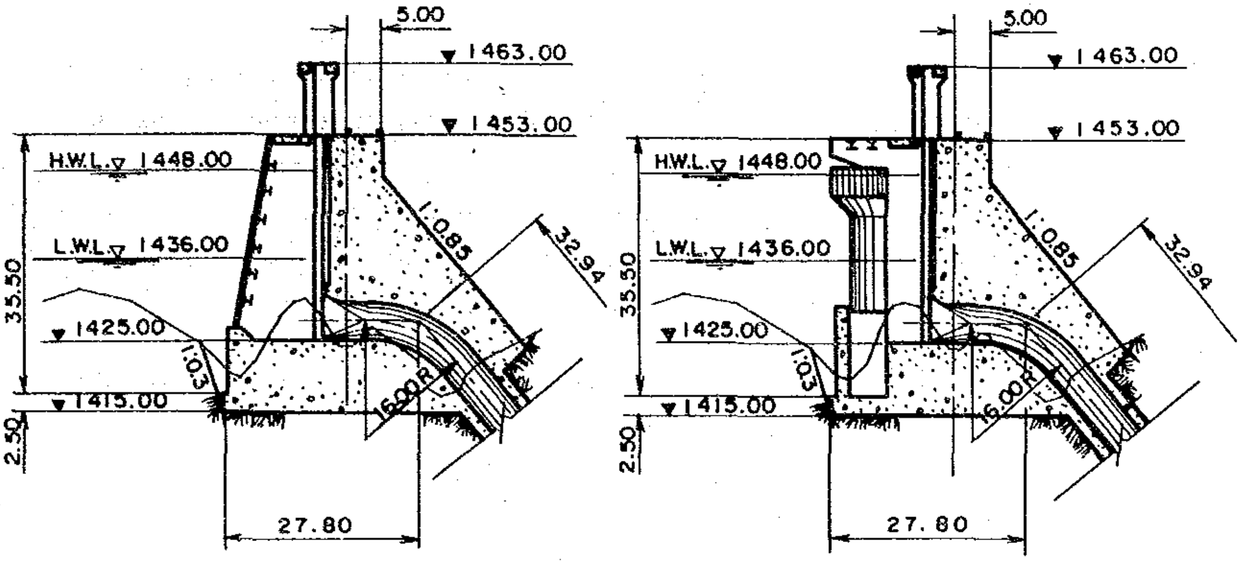

(A) Normal Type (B) Surface Intake Type

7.2.2 Structure in General

1) Location of Intake

The location of the intake is to be directly in the dam for the reasons given below.

(i) The right abutment of the dam is very steeply sloped, and if the intake were to be provided there, the civil works construction cost required for excavation, concrete, etc. will be increased, and it will be more economical to install the intake structure directly in the dam.

(ii) By installing the intake immediately by the side of the sand flush gate in the dam it will be possible to minimize the influence of sedimentation.

(iii) The effect of suspended load on the intake is the same whether at the right abutment of the dam or immediately in front of the dam it self.

2) Screen, Surface Intake Gate, and Regulating Gate By installing the screen above the surface intake gate and by reducing flow velocity through the screen to below V = 1.0 m/sec the load from the screen to the surface intake gate was alleviated.

The surface intake gate has a complex construction and water-tightness mechanism, so that by adopting a system to balance internal and external pressures without causing the gate to bear the full water pressure of the reservoir, the weight of the gate was made smaller for a construction capable of easily following the variation in water level.

The intake regulating gate was made to have a construction that it could be closed irrespective of the reservoir water level for inspection of structures from headrace to powerhouse or when there is an accident.

The sediment material shall be flushed out through the two sand flush gates when the sediment surface elevation in front of the intake structure reaches to 1,430.00 m at most, of which elevation is designed as the concrete crest of the intake structure.

The sediment material is not considered to be deposited at the inside of intake structure, however, the high water pressure flushing device with pipe and valve will be installed at the bottom of intake structure and the flushing pipe will be connected with that of the flushing gate. A drainage pipe line system is also adoptable for this purpose. This kind of study is, however, recommendable to be considered at the stage of definite study.

Furthermore, Japan has and maintains the same kind of intakes, but any problem has not yet happened.

7.3 Headrace Tunnel

7.3.1 Selection of Headrace Tunnel Route

The headrace tunnel route is to be selected as shown in Fig. 7-9 to obtain the most economical route on comparison studies of tunnel routes between work adits in the vicinity of the dam and work adits to be provided in the vincinity of the surge tank.

Providing a work adit approximately 2.0 km upstream from the surge tank and calculating total construction costs taking into account construction costs and interest amounts during the construction periods for Case I to case V , the results are as shown in Table 7-7.

Fig. 7-9 Headrace Tunnel Route

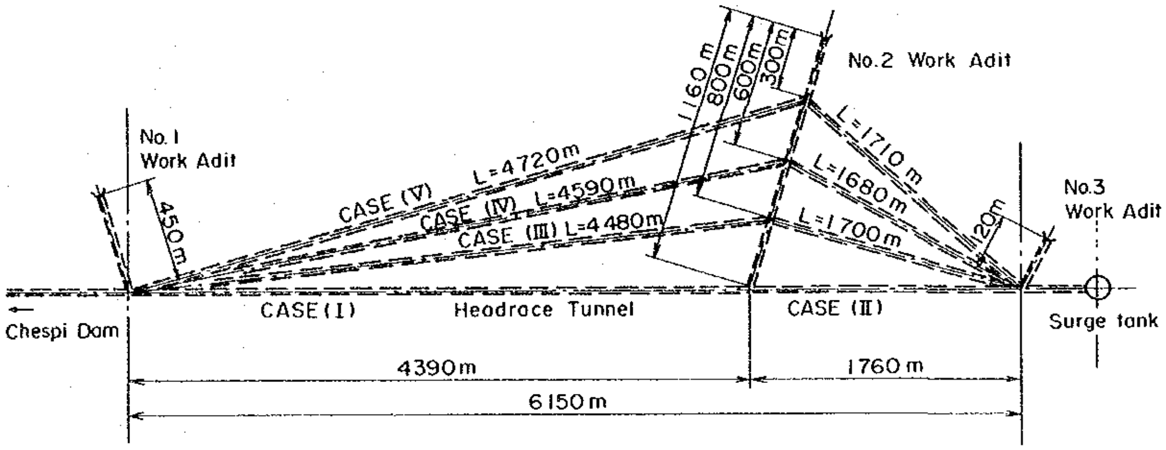

In comparisons of construction periods, it was assumed that excavation would be by ordinary methods for 110 m per month and lining concrete 145 m per month in all cases.

Based on the above results, the route of the headrace tunnel is to be the most economical straight line of Case 1 connecting the work adit in the vicinity of the dam and the surge tank.

Table 7–7 Comparison of Headrace Tunnel

	Construction Cost (C) 10^3US$	Term of Construction (t) Year	Intereest (T) T = 0.4 CRl	Total Cost 10^3US$
Cose I	51 067	4 733	9 668	60 735
Cose II	53 854	4 081	8 791	62 645
Cose III	53 533	3 958	8 475	62 008
Cose IV	53 658	3 881	8 330	61 988
Cose V	54 300	3 850	8 362	62 662

7.3.2 Determination of Inside Diameter of Headrace Tunnel

Determination of inside diameter of the headrace tunnel was done selecting the size at which the sum of the annual cost for the construction cost per unit length according to inside diameter and the annual electricity revenue loss due to head loss according to inside diameter would be a minimum. As a result of selection, D = 5.20 m is the most economical inside diameter as shown in Fig. 7-10.

7.3.3 Other Matters

Regarding the headrace tunnel, the following designs were made regarding matters other than route selection and determination of inside diameter.

(i) For a section of approximately 200 m in the vicinity of the intake where earth cover is thin, the structure is to be such that the design internal pressure would be borne with steel liners.

(ii) For the loosened zone of the surrounding natural ground resulting from headrace tunnel excavation, grouting is to be done with eight grout holes per cross section and 3.0-m length per hole at 3.0-m intervals after completion of lining concrete placement.

(iii) Approximately 20 m in the vicinity of the intersection between the No. 1 work adit and the headrace tunnel is to be provided with steel liner with a manhole installed for the purpose of future maintenance, while Work Adit No. 1 is to be left for liaison purposes.

(iv) Work Adit No. 2 is to be used in excavation work and in the main concrete lining work and is to be designed so that it will serve as a sand flushing facility in the future.

Table 7–8 Comparison of Construction Program (Headrace Tunnel)

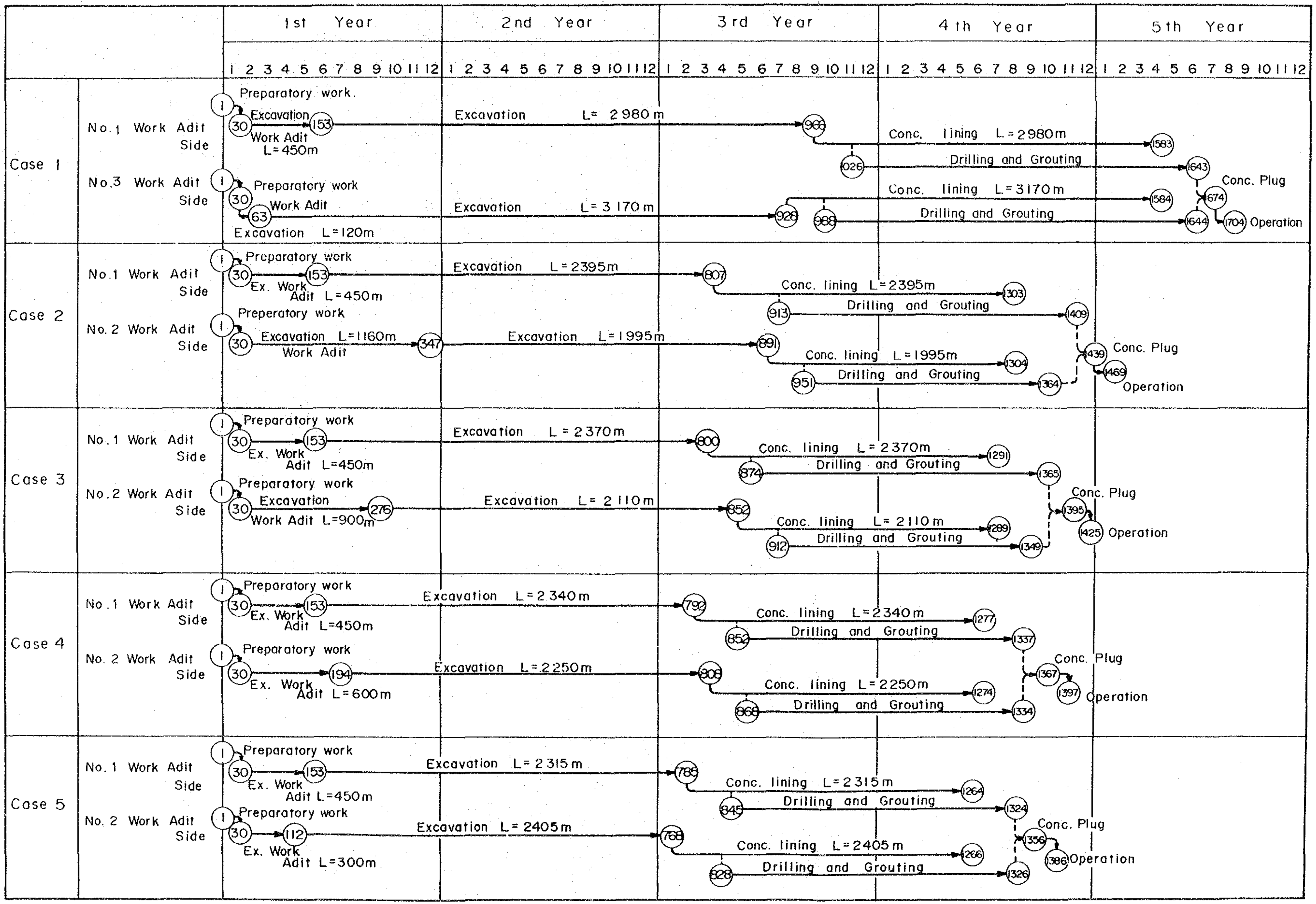

Fig. 7—10 Economic Diameter Diagram

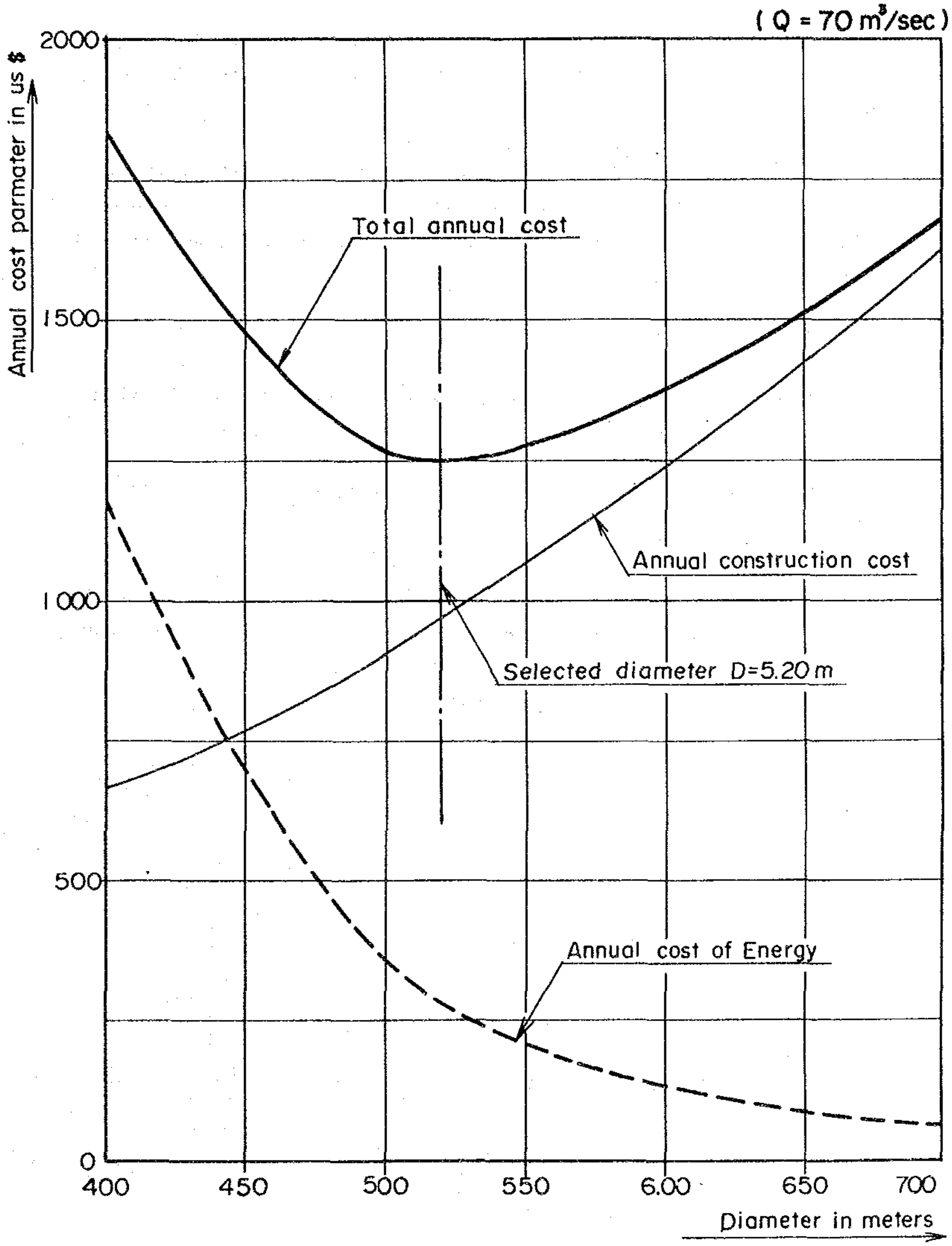

7.4 Surge Tank

7.4.1 Surge Tank, General

The surge tank is to be an orifice type considering the topographical and geological conditions, and is to be of a design having an upper chamber.

The inside diameter of the vertical shaft and the orifice diameter were determined making calculations to satisfy the conditions below, with the results being 8.0 m for vertical shaft inside diameter, and 2.1 m for orifice diameter.

(i) Study on critical flow of orifice

(ii) Study on optimum orifice diameter for load rejection and sudden increase in load.

(iii) Study on stability under dynamic vibrations

7.4.2 Surging Calculations

Surging was calculated using the specifications given in Fig. 7-11. The reservoir water level used is high water level at full load rejection and low water level at half-load demand.

Fig. 7-11 Surge Tank

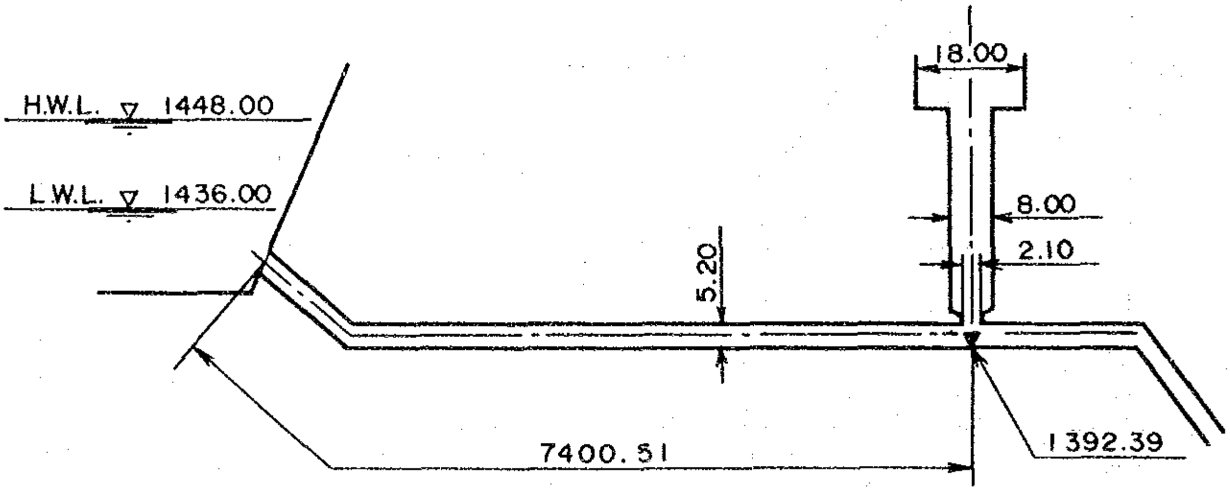

1) Fundamental Equation

$$\frac{dV}{dT} = \frac{z - \varepsilon \cdot \left| V \right| \cdot V - K}{L/g}$$

$$\frac{dz}{dt} = \frac{Q - f.V}{F}$$

$$K = \phi \cdot \left| Q \right| \cdot Q$$

where,

z: surge tank water level (reservoir water level 0 with downward direction as positive

V: flow velocity in headrace tunnel (m/sec)

f: cross-sectional area of headrace tunnel (m^2)

L: length of headrace tunnel (m)

F: cross-sectional area of surge tank (m^2)

ε: headrace tunnel head loss coefficient

Q: flow at surge tank base (m^3/sec)

K: orifice resistance

ϕ: orifice loss coefficient

2) Fundamental Values

Headrace tunnel

$f = 21.24\ m^2$, $L = 7{,}400.51$ m

Surge tank

$F_1 = 50.26\ m^2$ (D = 8.00 m)
$F_2 = 254.47\ m^2$ (D = 18.00 m)

Orifice Loss Coefficient

At inflow 0.9

At outflow 0.5

At load Rejection

Closing time Tl = 6 sec, Q = 70 m^3/sec → 0

Riservoir water level 1,448.00 m

At half-load demand

Opening time Tl = 3 sec, Q = 35 m^3/sec → 70 m^3/sec

Reservoir water level 1,436.00 m

Headrace head loss coefficient $\mathcal{E}$ down = 1.171355

3) Results of Calculations

Numerical calculations were made by the Runge-Kutta numerical integration method at 0.5-sec intervals using an IBM/S370-M155 electronic computer. The results are as shown in Fig. 7-12.

Fig. 7–12 Surging Curve

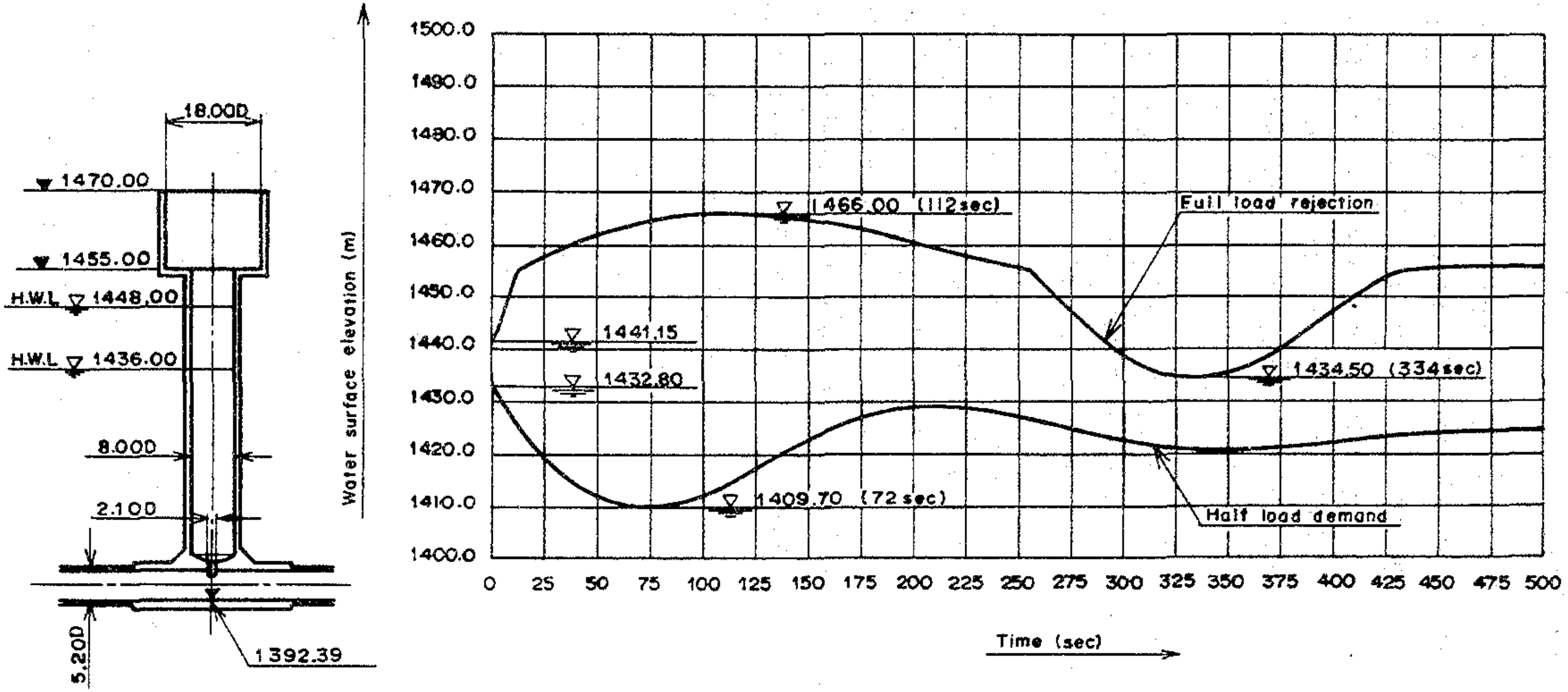

In the case of full load rejection

$Q = 70 m^3/sec \longrightarrow 0 m^3/sec$

$n = 0.011$

$\epsilon up = 0.630098$

Reservoir water surface = 1 448.00^m

In the case of half load demand

$Q = 35 m^3/sec \longrightarrow 70 m^3/sec$

$n = 0.015$

$\epsilon down = 1.171355$

Reservoir water surface = 1 436.00^m

7.5 Penstock

7.5.1 Selection of Penstock Route

The penstock route is to be decided on together with the powerhouse location. Taking into consideration the extremely rugged topography at this site, the two routes, 4 cases shown in Fig. 7-13 are conceivable as economical routes where the geological conditions are such that there are no faults or risk of slopes excavations for structures collapsing, while maintenance and administration will be easy.

On comparison studies of the two routes, four cases, Route I , Case 1 is the most economical as shown in Tables 7.9. This case has the following advantages compared with the others:

(i) At present, an access road axists to the powerhouse site for the purpose of investigation works, and the geological conditions have been thoroughly grasped through observations of slopes at excavations and results of boring works, and there are no factors for problems to arise during construction or in maintenance and administration.

(ii) Maintenance and administration will be easy because of the existence of this access road.

Fig. 7—13 Route of Penstock

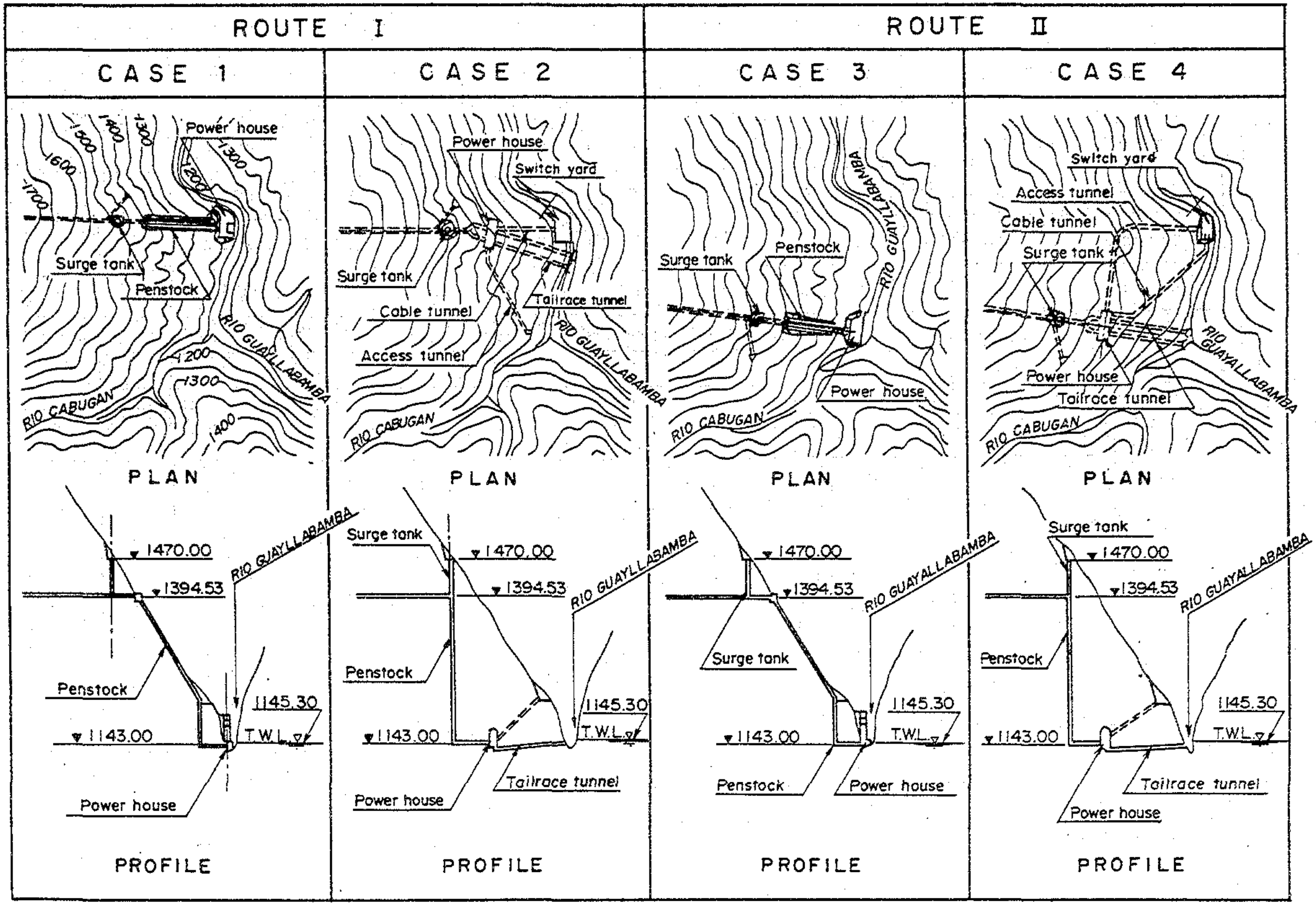

Table 7–9 Economic Comparison of Powerhouse Site and Type of Turbine

Case (I) — 1

Unit : 10^3 US $

Type turbine	Unit	Civil works							Electrical works	Total cost
		Penstock	Power house	Tailrace tunnel	Access tunnel	Cable tunnel	Switchyard	Total		
Francis type	2	10984	10208	0	0	0	0	21192	31 158	52 350
	3	11 517	11 719	0	0	0	0	23236	35 008	58 244
	4	12162	13775	0	0	0	0	25937	39238	65 175
Pelton type	2	11151	11 741	0	0	0	0	22892	36 396	59 288
	3	11651	14021	0	0	0	0	25672	42 483	68 155
	4	12 058	14640	0	0	0	0	26698	50092	76 790

Case (I) — 2

Type turbine	Unit	Civil works							Electrical works	Total cost
		Penstock	Powerhouse	Tailrace tunnel	Access tunnel	Cable tunnel	Switchyard	Total		
Francis type	2	7 005	8476	6523	2648	1 073	1 831	27 556	31 713	59 269
	3	7696	9538	8 399	2478	1 033	1 934	31 078	36 021	67 099
	4	8 351	10463	9 392	2232	1 055	2 040	33 533	40 654	74 187
Pelton type	2	7 131	13858	4995	3 115	1 033	1 831	31 963	36 783	68 746
	3	8369	15681	5660	2737	974	1 934	35355	43 375	78 730
	4	8 556	14484	5856	2562	1 055	2040	34553	51 429	85 982

7.5.2 Determination of Inside Diameter of Penstock

The inside diameter of the penstock was selected so that the sum of the annual cost for the construction cost per unit length according to inside diameter and the annual electricity revenue loss due to head loss according to inside diameter would be a minimum

As the condition for determining the inside diameter, calculations were made with the centroidal distance considering bifurcation converted to elevation of 1,250.00 m as the reference cross section. As a result of the calculations, D = 3.60 m was found to be the most economical as shown in Fig. 7-14. With this D = 3.60 m as the basis, the diameter is to be gradually reduced in the direction of the powerhouse to inside diameter of D = 2.10 m at the connections with casings, while in the direction of the surge tank, it is to be gradually enlarged to the inside diameter of the headrace tunnel of D = 5.20 m.

7.5.3 Bifurcation Location of Penstock and Steel Used

The location of bifurcation of the penstock would be most economical if it were to be immediately upstream of the powerhouse when considerations are given including civil works construction cost, and the method of bifurcation is to be Escher wyss type to minimize head loss as much as possible. The steel used is to be SM-58 class.

Fig. 7–14 Economic Diameter Diagram

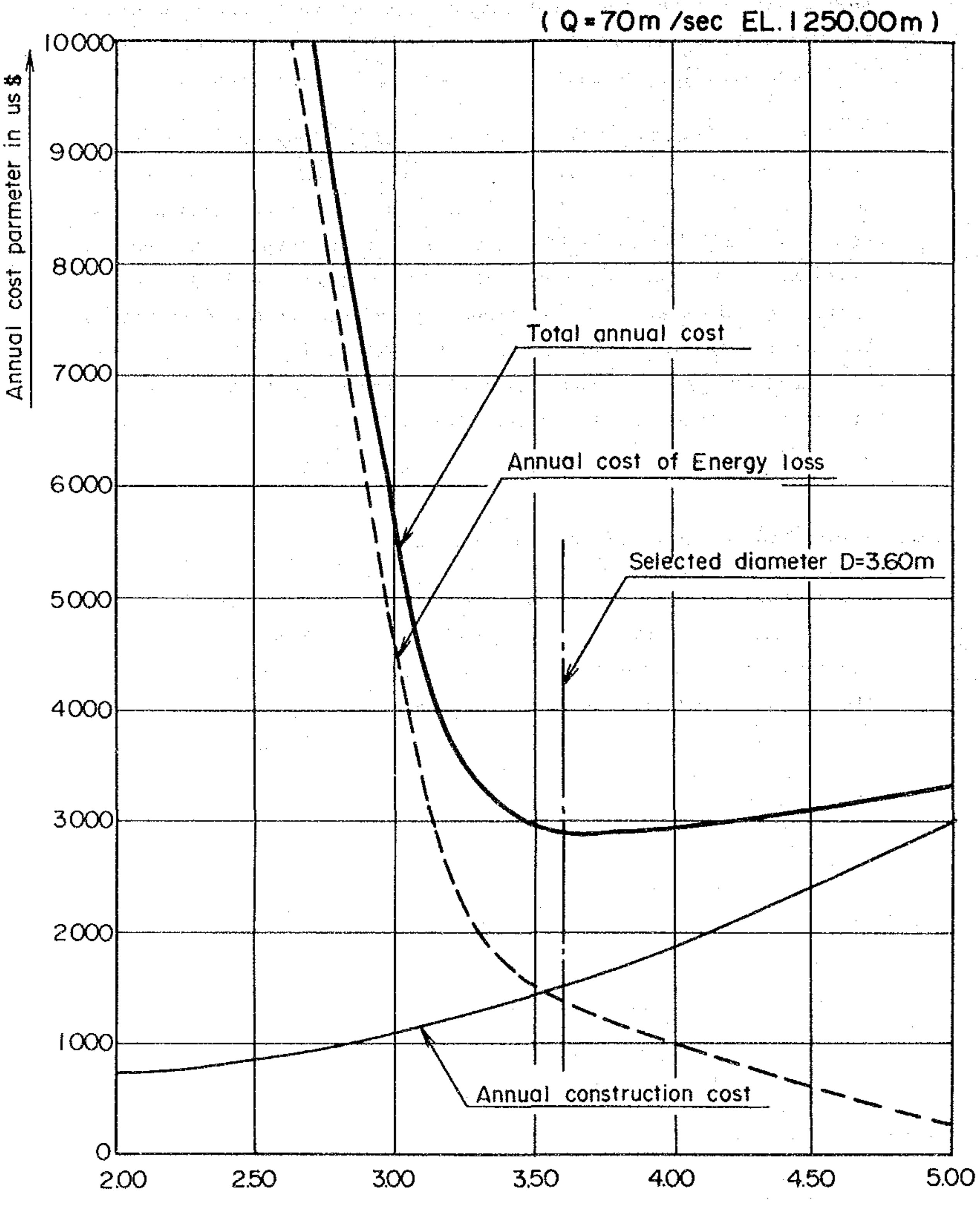

7.5.4 Calculation of Water Hammer

1) Outline

The penstock is to be in the form of one line from the base of the surge tank to immediately upstream of the powerhouse, partly embedded in a tunnel and partly as a surface penstock, bifurcated, and connected to turbines.

2) Calculation Method

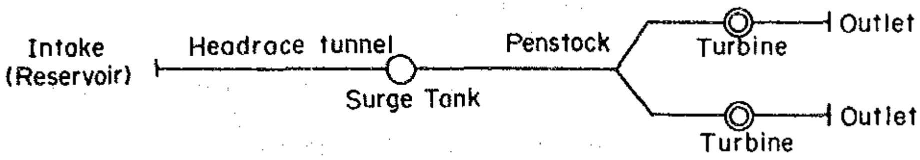

The variations in pressure and quantity of flow occurring in the waterway system shown in the above diagram when the degree of opening of turbine guide vanes are changed are discussed in the following clause.

The fundamental equation is obtained by successive approximation at intervals of 0.01 sec. The degree of opening of guide vanes is assumed to vary linearly, with head loss produced concentrated at the end of the conduit assumed and calculated based on actual conduit length. The value computed is also to include the influence of surging.

3) Fundamental Equation

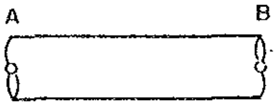

The fundamental equation for calculation of pressure waves in a simple conduit waterway as shown in the above diagram is as given below.

$$H_A,(t) \pm S.QA,(t) = H_B,(t-\frac{L}{a}) \pm S.QB,(t-\frac{L}{a})$$

where,

H_A (t): pressure at point A at time t

Q_A,(t): flow quantity at point A at time t

$H_B,(t-\frac{L}{a})$: pressure at point B at time $t-\frac{L}{a}$

$Q_B,(t-\frac{L}{a})$: flow quantity at point B at time $t-\frac{L}{a}$

S: constant $= \frac{a}{g.A}$

a: propagation velocity of pressure wave in conduit

g: acceleration of gravity

A: cross-sectional area of conduit

L: length of conduit

4) Boundary Condition

(i) Boundary Condition at Closing Device

When performing linear closing at the closing device, in effect, the guide vane, the following boundary condition will hold ture.

$$Q_A,(t) = (1 - \frac{t}{T}) \cdot \sqrt{H_A(t) - H_B,(t)}$$

where,

t: any time within closing time of closing device $(0 \leqq t \leqq T)$

T: closing time of closing device

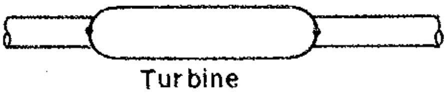

(ii) Boundary Condition at Bifurcation

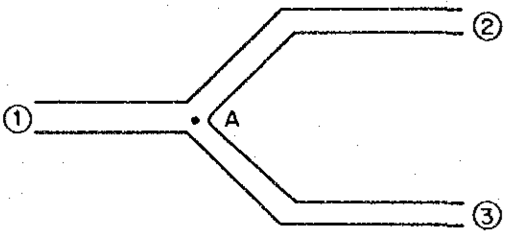

In bifurcation, the pressures of the three conduits are to be equal at point A, and the flows are to be continuous. That is, the boundary condition is to be that the following will be valid:

$$Q①,t = Q②,t + Q③,t$$

(iii) Boundary Condition at Intake (Reservoir)

The following boundary condition will be valid at the intake:

$$H_A,(t) = H_A,0$$

5) Fundamental Values

The values used in calculations are as follows:

(i) Headrace Tunnel

Length	7,400.51 m
Cross-sectional area	21.24 m^2 (D = 5.20 m)

(ii) Surge Tank

Upper chamber bed elevation	EL. 1,455.00 m
Upper chamber cross-sectional area	254.47 m^2 (D = 18.00 m)
Vertical Shaft cross-sectional area	50.26 m^2 (D = 8.00 m)
Vertical shaft cross-sectional area	50.26 m^2 (D = 8.00 m)
Vertical shaft base elevation	EL. 1,397.59 m

(iii) Penstock

Surge tank - bifurcation	525.23 m
Bifurcation - Turbine No. 1	52.02 m
Bifurcation - Turbine No. 2	52.02 m

Cross-sectional area (equivalent cross-sectional area)

Surge tank - bifurcation	11.783 m^2 (3.86 m)
Bifurcation - Turbine No. 1	3.723 m^2 (2.18 m)
Bifurcation - Turbine No. 2	3.723 m^2 (2.18 m)

(iv) Tailrace

Length	16.22 m
Cross-sectional area	5.11 m^2

(v) Turbine

Maximum discharge	35.0 m^3/sec x 2 = 70 m^3/sec
Number of units	2
Center elevation	EL. 1,143.00 m
Closing time	6.0 sec

(vi) Pressure Propagation Velocity 1,000 m/sec

6) Calculation Results

Calculations were made for 0.01-sec intervals using an electronic computer. The results of calculations are as shown in Fig. 7-15.

The maximum value of water hammer shown as a ratio to hydrostatic pressure is as follows:

$$H_A,(5.74)/H_A,(0) = \frac{117.47}{305.00} = 0.385$$

Fig. 7—15 Penstock Water-Hammer

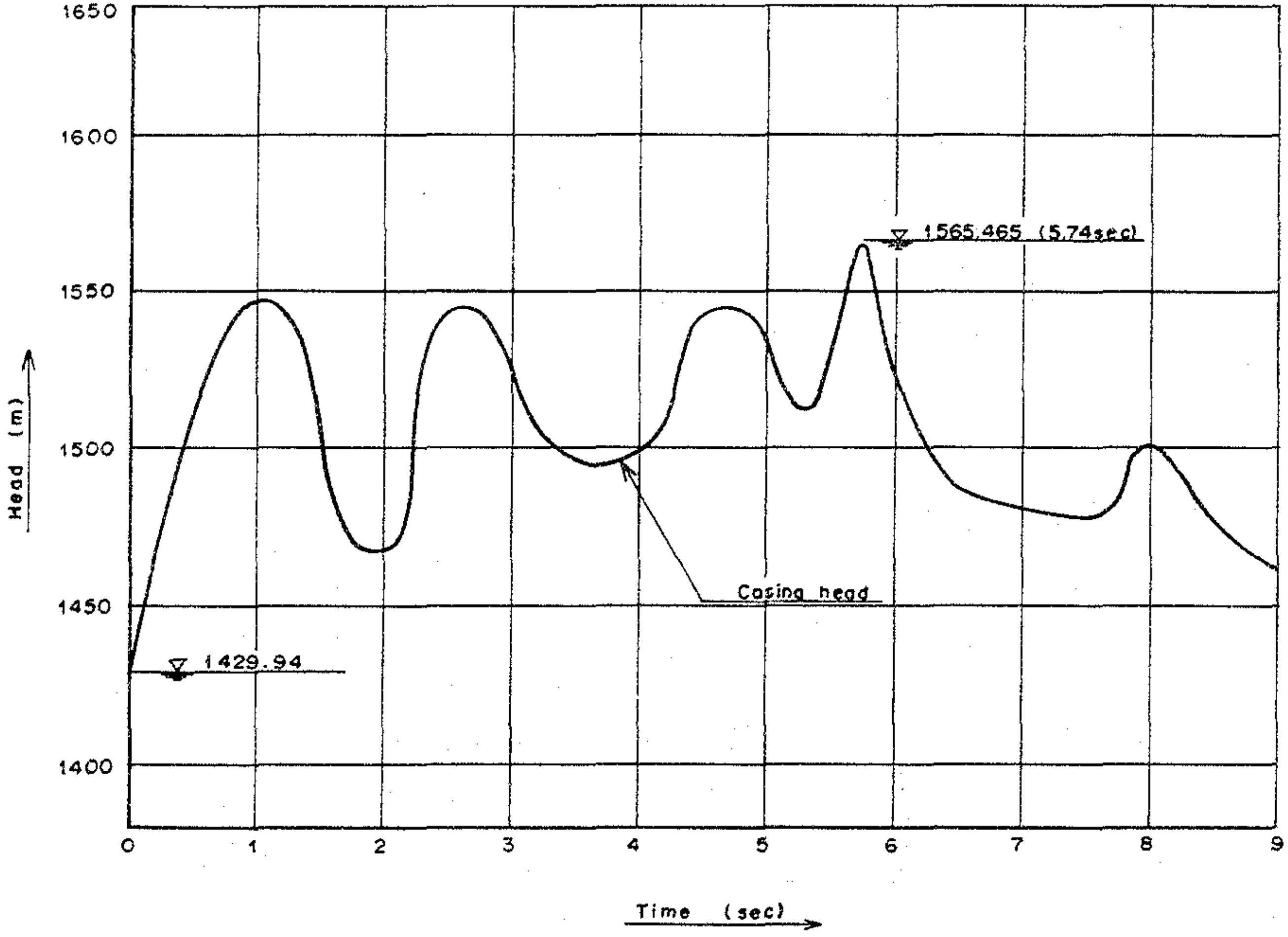

Reservoir water Surface elevation	1 448.00^{m}
Tailace water Surface elevation	1145.30
Maximum discharge	35m^3/sec× 2 =70m^3/sec
Number of generator	2 units
Closing time	6sec
Pressure wave Propagation velocity	1.000^{m}/sec

7.5.5 Strength Calculations of Penstock

1) Outline

The penstock is to be of welded steel plate, partially embedded and partially surface, and is to be designed to have ample strength against internal and external pressures.

The design internal pressure is to be computed based on the sum of hydrostatic pressure and pressure rise due to water hammer and surging. The design external pressure is to be taken as 4.0 kg/cm^2 at the embedded portion.

2) Study on Internal Pressure

(i) Design Heads and Major Points

Pressure rises from water-hammer action and surging, based on 7.5.4, "Calculation of Water Hammer," are to be approximately 40 percent of turbine center hydrostatic pressure, approximately 37 percent at the bifurcation, and approximately 7 percent at the base of the surge tank. Pressures at intermediate points are considered to vary linearly.

(ii) Calculation of Pipe Thickness

The pipe thickness is to be calculated by the equation below.

Tunnel Portion

$$\sigma = \frac{PD(1-\lambda)}{2(t-\varepsilon)y}, \quad t = \frac{PD(1-\lambda)}{2\sigma_a y} + \varepsilon$$

Surface Portion

$$\sigma = \frac{PD}{2(t-\varepsilon)y}, \quad t = \frac{PD}{2\sigma_a y} + \varepsilon$$

where,

σ: Circumferential stress of steel pipe (kg/cm^2)

P: acting internal pressure (kg/cm^2)

D: inside diameter of pipe (cm)

λ: pressure shared by bedrock (to be 20%)

t: pipe thickness (cm)

$\mathcal{E}$: corrosion allowance (= 0.15 cm)

y: longitudial direction welding efficiency (= 0.95)

σa: allowable stress of steel pipe (SM 58 σa = 2,400 kg/cm^2)

The minimum plate thickness is calculated by the following equation:

$$t = \frac{D + 800}{400} \text{ (mm)}$$

(iii) Calculation Results

The design head of the penstock and pipe shell thickness are shown in Fig. 7-16.

Fig. 7–16 Steel Penstock Design Head Diagram

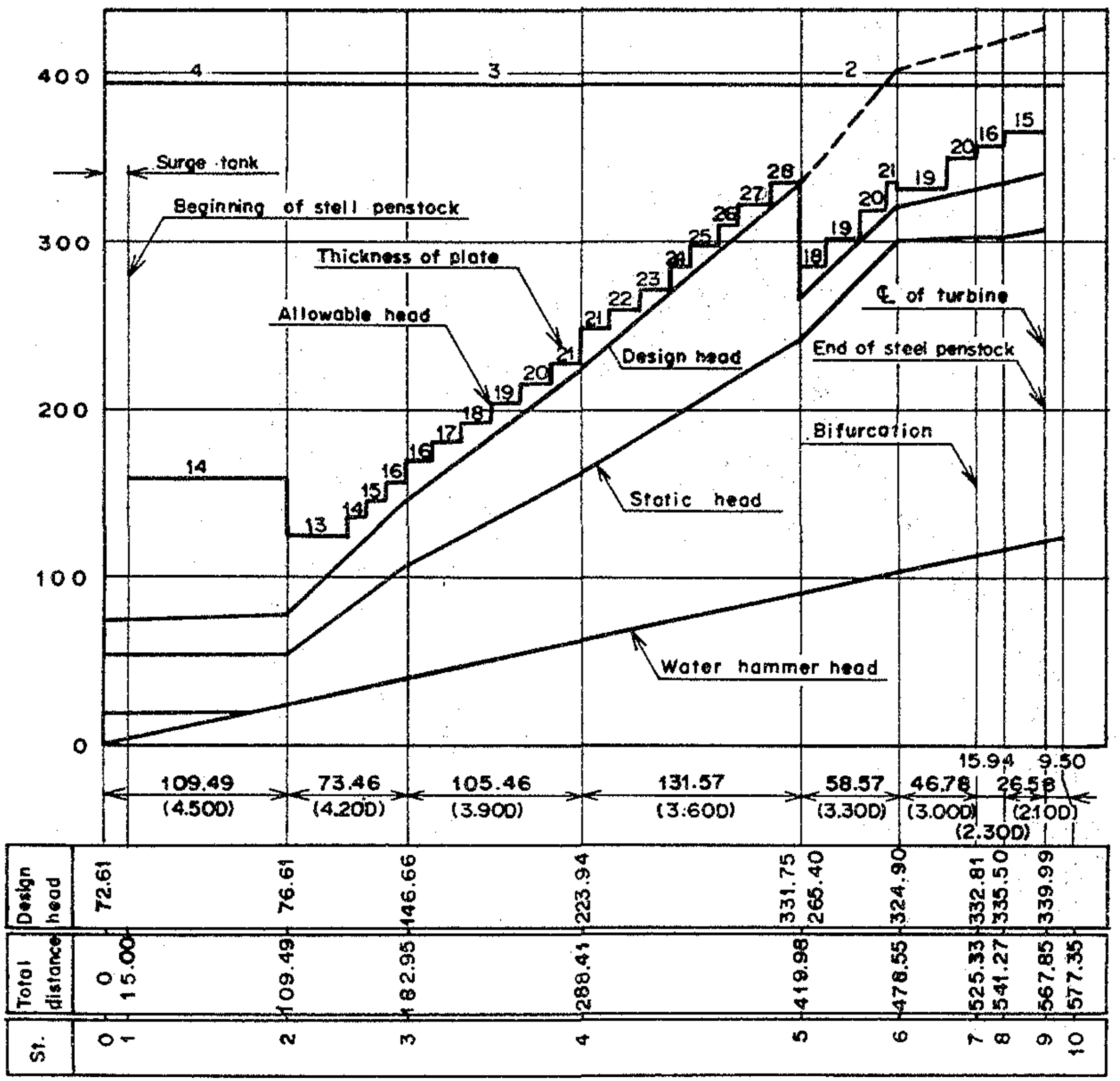

Speification

Maximum discharge	70m³/sec
Maximum static head	305.00m
Water hammer (at turbine)	122.00m
Closing time	6.0 sec
Material	
Allowable tensile stress	2400 kgf/cm²
Weldig efficiency	95 %
Corrosion allowanse	1.5mm

3) Study on External Pressure

(i) Calculation Principle

Whether or not stiffeners are necessary against design external pressure shown in the diagram is calculated, and when stiffeners are required, calculations are to be made for the stiffeners assumed.

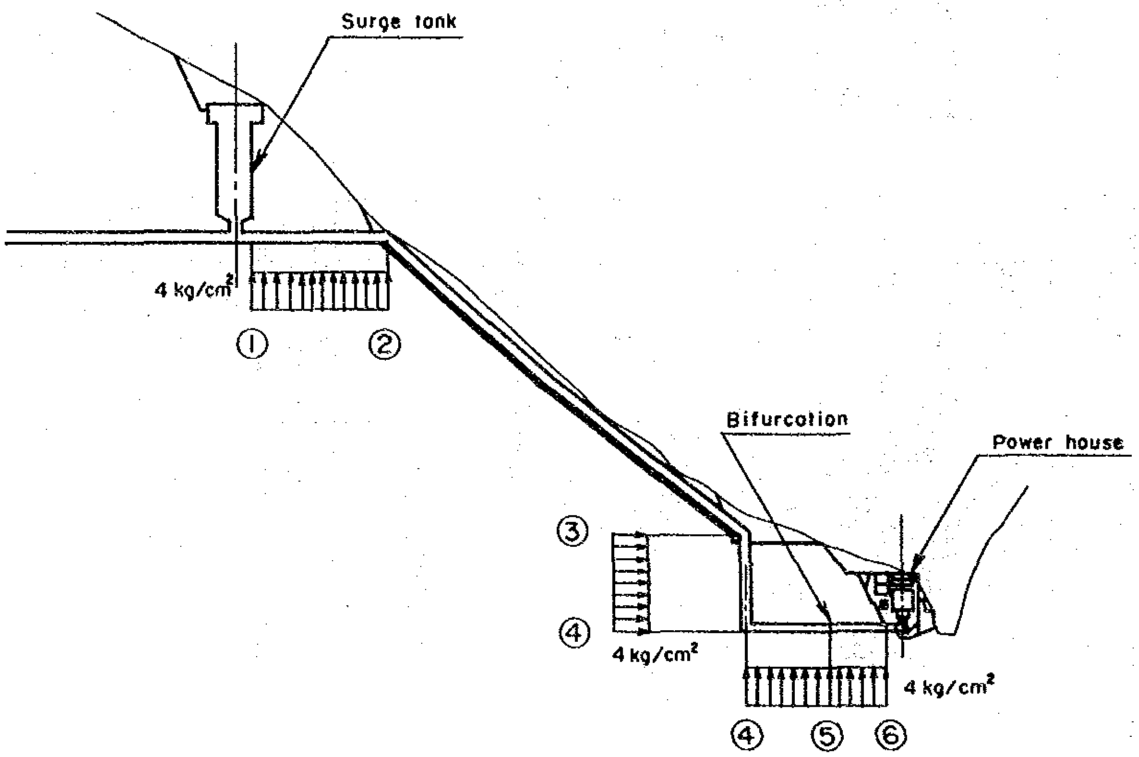

(ii) Critical Buckling stress in Case of No Stiffener

Calculations are made by E. Amstutz's equation.

$$\left(\frac{Ko}{rm} + \frac{\sigma N}{E_s*}\right)\left(1 + 12\frac{rm2}{t2}\cdot\frac{\sigma N}{E_s*}\right)^{1.5}$$

$$= 3.36\ \frac{rm}{t}\cdot\frac{\sigma F* - \sigma N}{E_s*}\cdot\left(1 - 1/2\frac{\sigma m}{t}\cdot\frac{\sigma F* - \sigma N}{E_s*}\right)$$

where,

Ko: gap between concrete and outer surface of pipe

$$= 5.2 \times (\frac{Do}{2} + t + \varepsilon)/10{,}000 \text{ (cm)}$$

rm: $\frac{Do + t + \varepsilon}{2}$ (cm)

σN: circumferential-direction stress of pipe shell plate at part where deformation occurred (kg/cm^2)

$E_s{}^*$: $\frac{Es}{1 - \nu^2}$

t: pipe shell thickness

σF^*: $\mu \cdot \frac{F}{\sqrt{1 - \nu + \nu^2}}$

ν : poisson's ratio (= 0.3)

μ: $1.5 - 0.5 \times \frac{1}{(1 + 0.002 \cdot \frac{Es}{\sigma F})^2}$

σF: yield point stress of material = 4,600 kg/cm^2

The results of calculations according to the above are as given in the Table below.

Sta.	Diameter cm	Thickness cm	External Pressure kg/cm²	External pressre (with safety factor 1.5)	Critical buckling stress kg/cm²	Stiffeners	Note
①	450	1.4	4.0	6.0	4.6	Yes	
②	450	1.4	4.0	6.0	4.6	〃	
③	330	1.8	4.0	6.0	15.2	No	
④	315	1.9	4.0	6.0	20.6	〃	
⑤	230	1.6	4.0	6.0	24.5	〃	
⑥	210	1.5	4.0	6.0	25.7	〃	

(iii) Critical Buckling Stress in Case of Necessity for Stiffener

iii-1) Critical Buckling Stress of Pipe Shell Proper

(s. Timoshenko's Equation)

$$\frac{(1-\nu s^2)r_o'P_K}{Es.t} = \frac{1-\nu s^2}{(n^2-1)\left(1+\frac{n^2\ell^2}{\pi^2 r_o^2}\right)} + \frac{t2}{12r_o'2}$$
$$\cdot\left\{(n^2-1)+\frac{2n^2-1-\nu s}{1+\frac{n^2\ \ 2}{\pi^2 ro'^2}}\right\}$$

where,

PK: critical buckling stress (kg/cm^2)

Es: modulus of elasticity (2.1 x 10^6 kg/cm^2)

νs: Poisson's ratio (0.3)

t: pipe thickness (cm)

n: number of wrinkles

r_o': radius to outer surface of pipe (cm)

ℓ: interval between stiffeners

iii-2) Critical Buckling Strength of Stiffener

(E. Amstutz's Equation)

$$\left(\frac{Ko}{rm}+\frac{\sigma cr}{Es}\right)\left(1+\frac{rm2}{12}.\frac{\sigma cr}{Es}\right)^{1.5}$$
$$= 1.68\frac{rm}{e}.\frac{\sigma F-\sigma cr}{Es}\left(1-1/4.\frac{rm}{e}.\frac{\sigma F-\sigma cr}{Es}\right)$$

where,

σcr: critical buckling stress of stiffened portion (kg/cm^2)

σF: yield point stress of material (4,600 kg/cm^2)

K_o: gap between concrete and outer surface of pipe

$= 5.2 (\frac{Do}{2} + t + \varepsilon)/10,000$ cm

E_s: elastic modulus of steel (2.1×10^6 kg/cm^2)

R_m: $\frac{Do + t + \varepsilon}{2}$ (cm)

i: rotation radius of synthesized cross section of stiffener (cm)

e: distance from centroid of synthesized cross section of stiffener to inner surface of pipe (cm)

Effective Width of pipe Shell Plate

b_o: $1.56 \sqrt{rm.t} + b$

where,

b_o: effective width of pipe shell plate (cm)

rm: pipe radius (cm)

t: pipe shell thickness (cm)

b: thickness of stiffener web (cm)

Average Compressive Stress of Stiffener

$$\sigma c = \frac{Po.ro.bo}{So + 1.56t\sqrt{rm.t}}$$

where,

Po: converted external pressure

So: cross-sectional area of stiffener (= b(t+h))

iii-3) Calculation Results

The results of calculations are as shown below.

Stiffeners will be required between measurement points ① and ② and if stiffeners of the kind illustrated below are used at every 2.00 m, the critical buckling strength will be P_K = 7.61 kg/cm^2 for the pipe shell proper, and σcr = 3,728.50 kg/cm^2 for the stiffener. Hence, $\sigma cr/\sigma c$ = 4.55

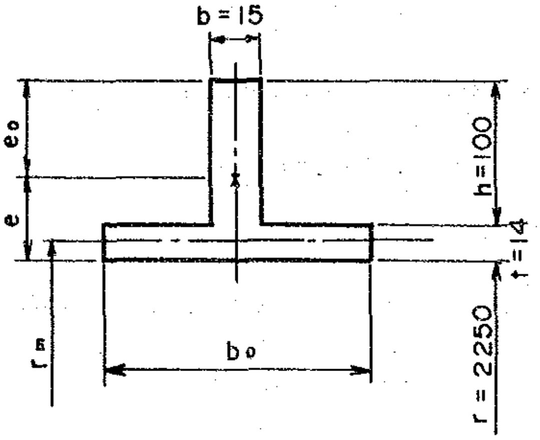

7.6 Powerhouse

It is necessary for a powerhouse location, the type of turbine to be installed there, and the number of turbines to be decided on not considering the powerhouse alone, but examining it as an overall structure including the waterway system consisting of the penstock and part downstream, access road, outdoor switchyard, etc.

Here, the two routes, four cases, as described in 7.5.1, "Selection of Penstock Route," are conceivable according to an overall judgment based on the results of field investigations, whether the topographical conditions are good or bad, and including maintenance and administration.

The results of economic comparisons of the individual cases are as shown in Table 7-9, with the Plan Route I , Case 1 being the most economical. The specifications, advantages and disadvantages of each case are described below.

i) Plan Route I , Case 1

i-1) Penstock

Branching according to the number of turbines would be as shown in Figs. 7-17, 7-18, 7-19, with comparison as shown in Table 7-10.

i-2) Powerhouse

The comparisons according to types of turbines and numbers of units are as shown in Table 7-11.

i-3) Overall Penstock and Powerhouse Comparison

The overall comparison including penstock and powerhouse is as given below.

1 As shown in Table 7-10 and 7-11, the most economical turbine type and number of turbine units would be Francis type and two units.

2 The complexities of branching the penstock would be simplified most with a 2-unit scheme, and the tunnel portion would also be shorter.

3 If Pelton-type turbines were to be adopted it would be necessary for the distribution panel room, cable handling room, etc. to be provided in a building separate from the main powerhouse building.

4 The head loss with the Pelton turbine 2-unit scheme is approximately 1.10 m (H = 8.80 - 6.30 - 1.40) less than with the Francis turbine 2-unit scheme, which corresponds to approximately 700 kW when converted a power generation. However, with two Pelton turbines, the weights would exceed the transportation limits, and thus this scheme cannot be very well adopted.

ii) Plan Route I , Case 2

ii-1) Penstock

Branching according to the number of turbines would be as shown in Fig. 7-20, 7-21, 7-22, with comparison as shown in Table 7-12 to 7-16.

ii-2) Powerhouse and Appurtenant Structures

The comparisons according to types of turbines and numbers of units are as shown in Tables 7-13-1 to 7-13-4.

ii-3) Overall Penstock and Powerhouse Comparison

The overall comparison for this case is as given below.

1 When economic comparisons are made for the penstock and powerhouse independently they would cost less than in Case 1, but when an overall comparison is made adding appurtenant structures such as the tailrace tunnel, equipment delivery tunnel, etc., Case 1 would be more economical.

2 To take geological conditions into consideration, it is thought the underground powerhouse site has numerous cracks and it is necessary for the rock around the powerhouse to be reinforced.

iii) Plan Route II, Case 3

iii-1) Penstock and Powerhouse

Branching according to types of turbines and numbers of units are as shown in Figs. 7-17 to 7-19 with comparisons as shown in Table 7-14 to 7-15.

iii-2) Overall Penstock and Powerhouse Comparison

The overall comparison of this case is as given below.

1 When the topography and geology are considered, the amount of excavation at the powerhouse site will be especially large and this will not be more economical than Case 1.

2 The most economical scheme for this case would be for two Francis turbines. Compared with Case 1, the effective head would increase approximately 10 m. This corresponds to 3.6 percent in terms of output. However, the construction cost would be increased 18.4 percent, and Case 1 would be more economical.

iv) Plan Route II , Case 4

iv-1) Penstock and Powerhouse

Branching according to types of turbines and numbers of units are as shown in Figs. 7-20 to 7-22 with comparison as shown in Table 7-16 to 7-17.

iv-2) Overall Penstock and Powerhouse Comparison

The overall comparison of this case is as below.

In this case, the scheme for two Francis turbines would be advantageous, but as with Case 2, Case 1 is the most economical.

Fig. 7–17 Plan of Powerhouse Area of Francis Turbine Type

Case of 2 units

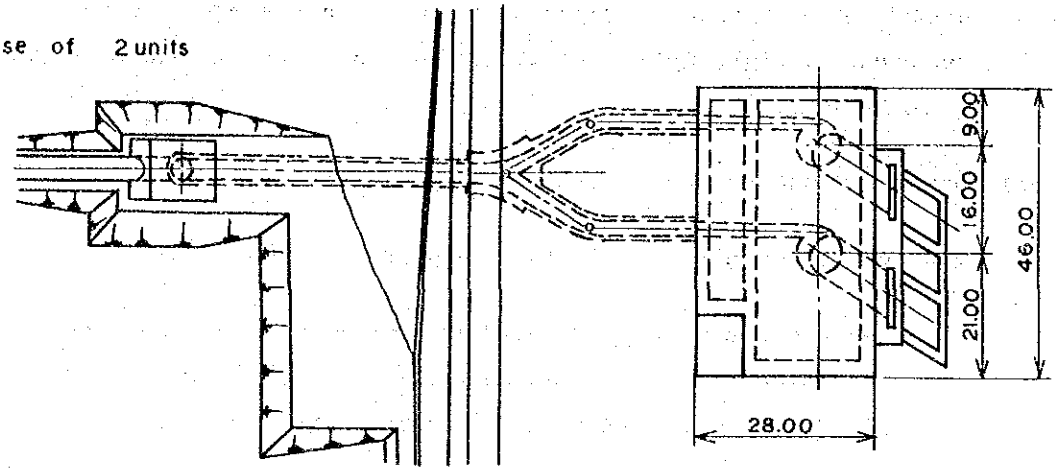

Case of 3 units

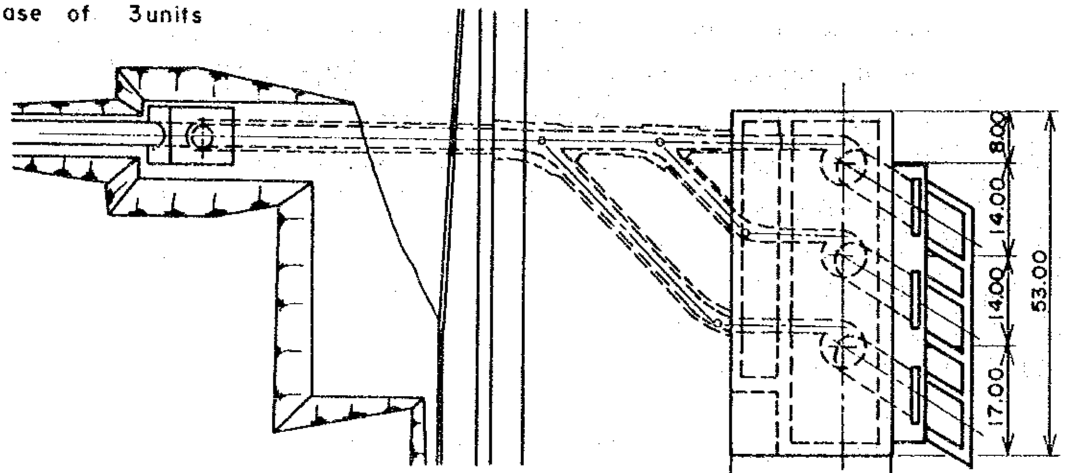

Case of 4 units

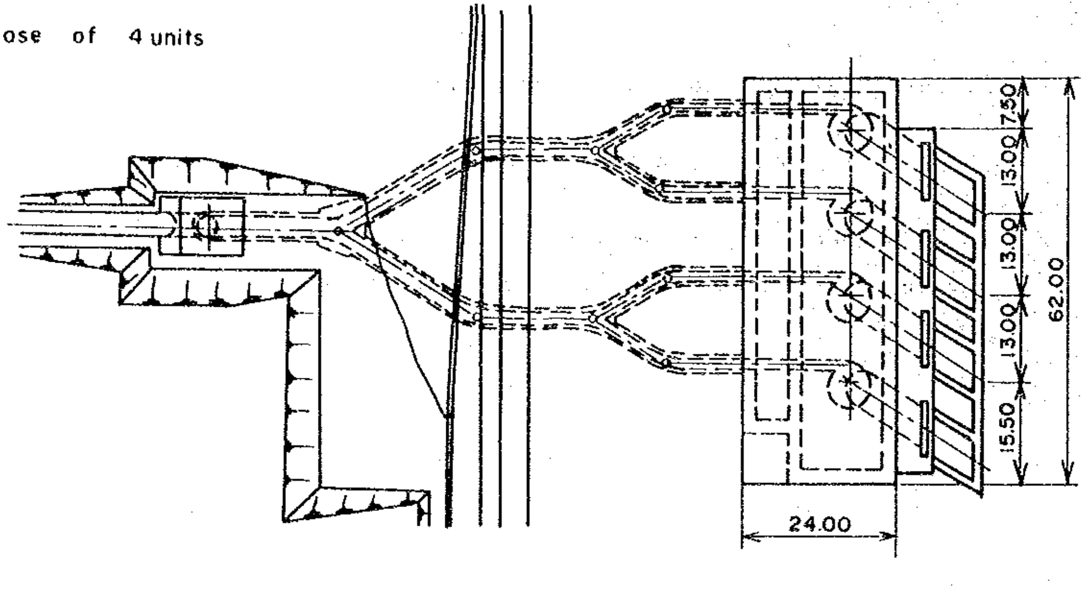

Fig. 7–18 Plan of Powerhouse Area of Pelton Turbine Type

Case of 2units

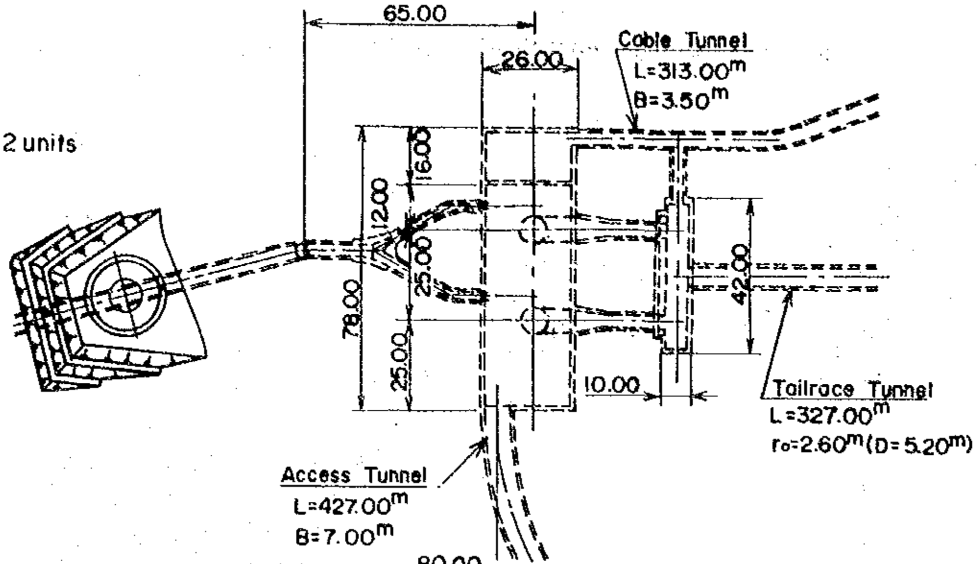

Case of 3units

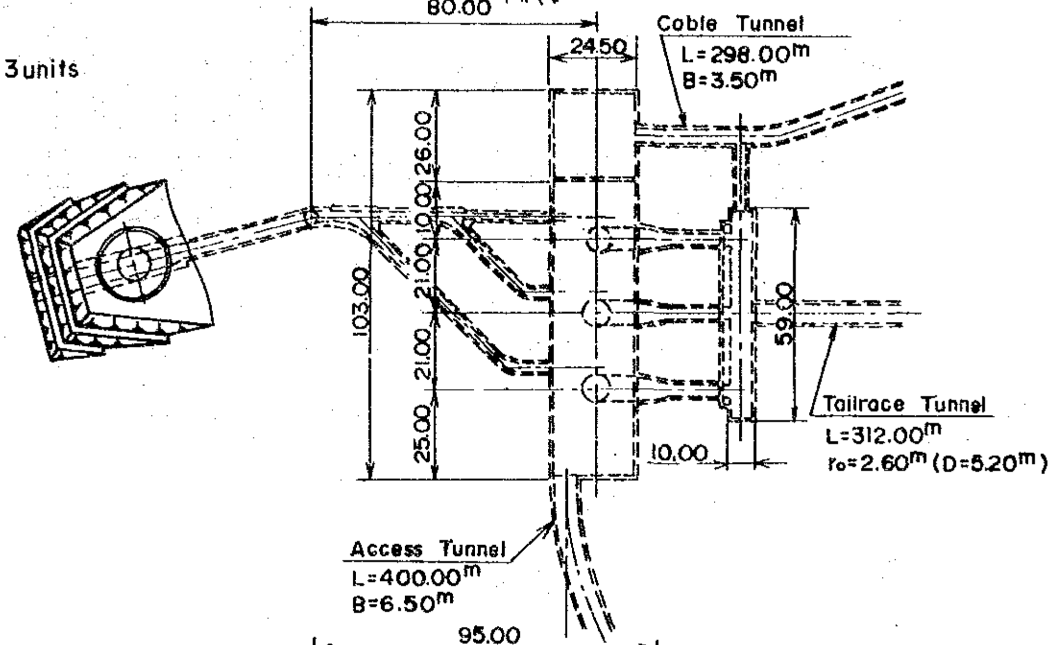

Case of 4units

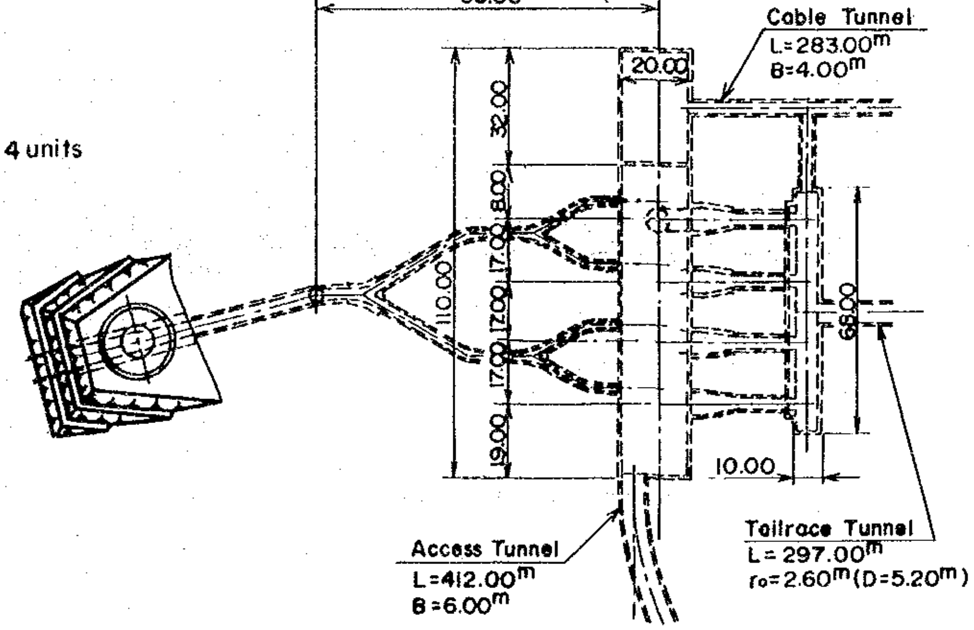

Fig. 7–19 Longitudinal Section of Each Turbine

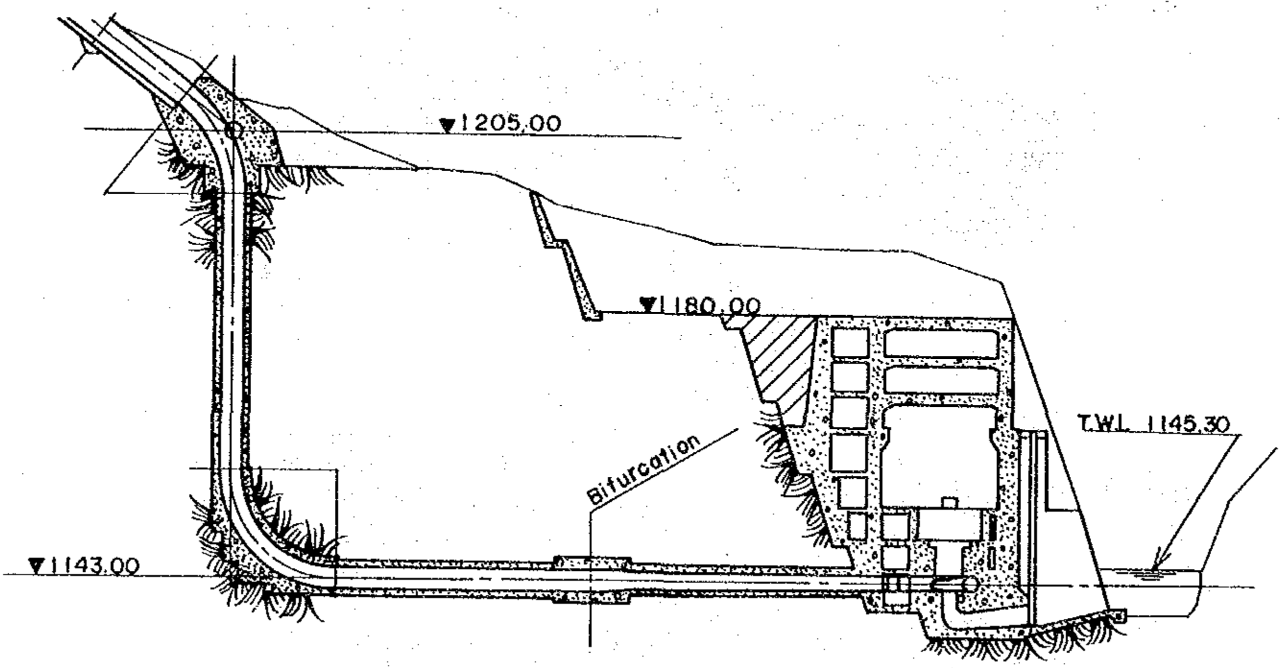

Francis turbine type (Case of 2 units)

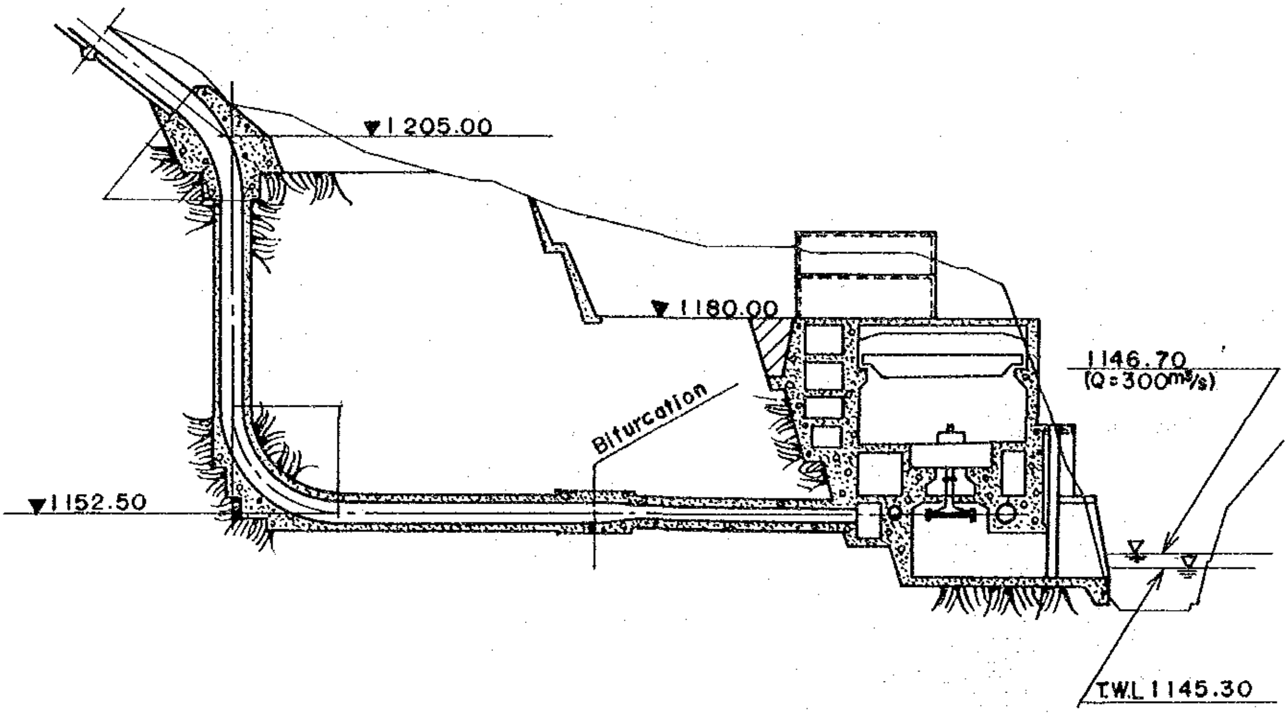

Pelton turbine type (Case of 2 units)

Fig. 7–20 Plan of Powerhouse Area of Francis Turbine Type

Case of 2unit

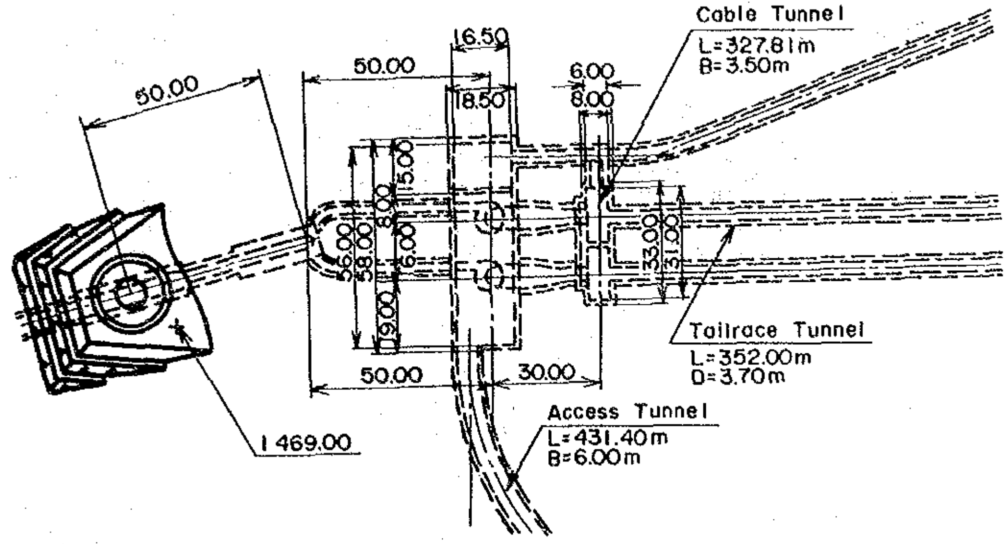

Case of 3unit

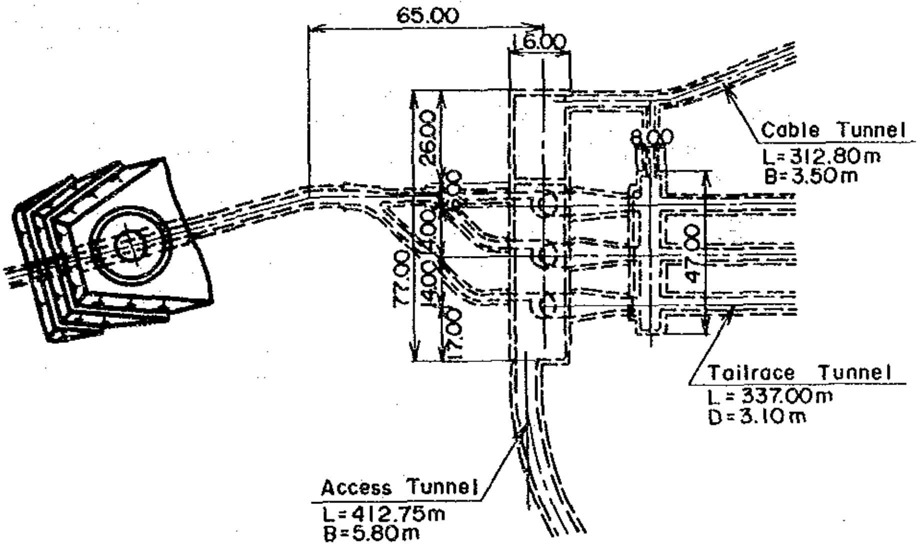

Case of 4unit

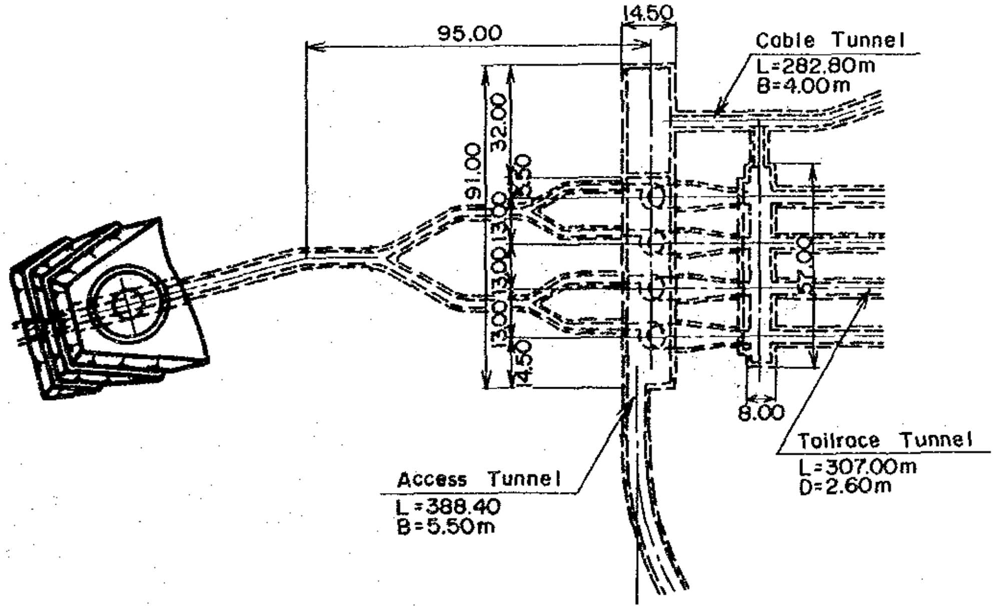

Fig. 7–21 Plan of Powerhouse Area of Pelton Turbine Type

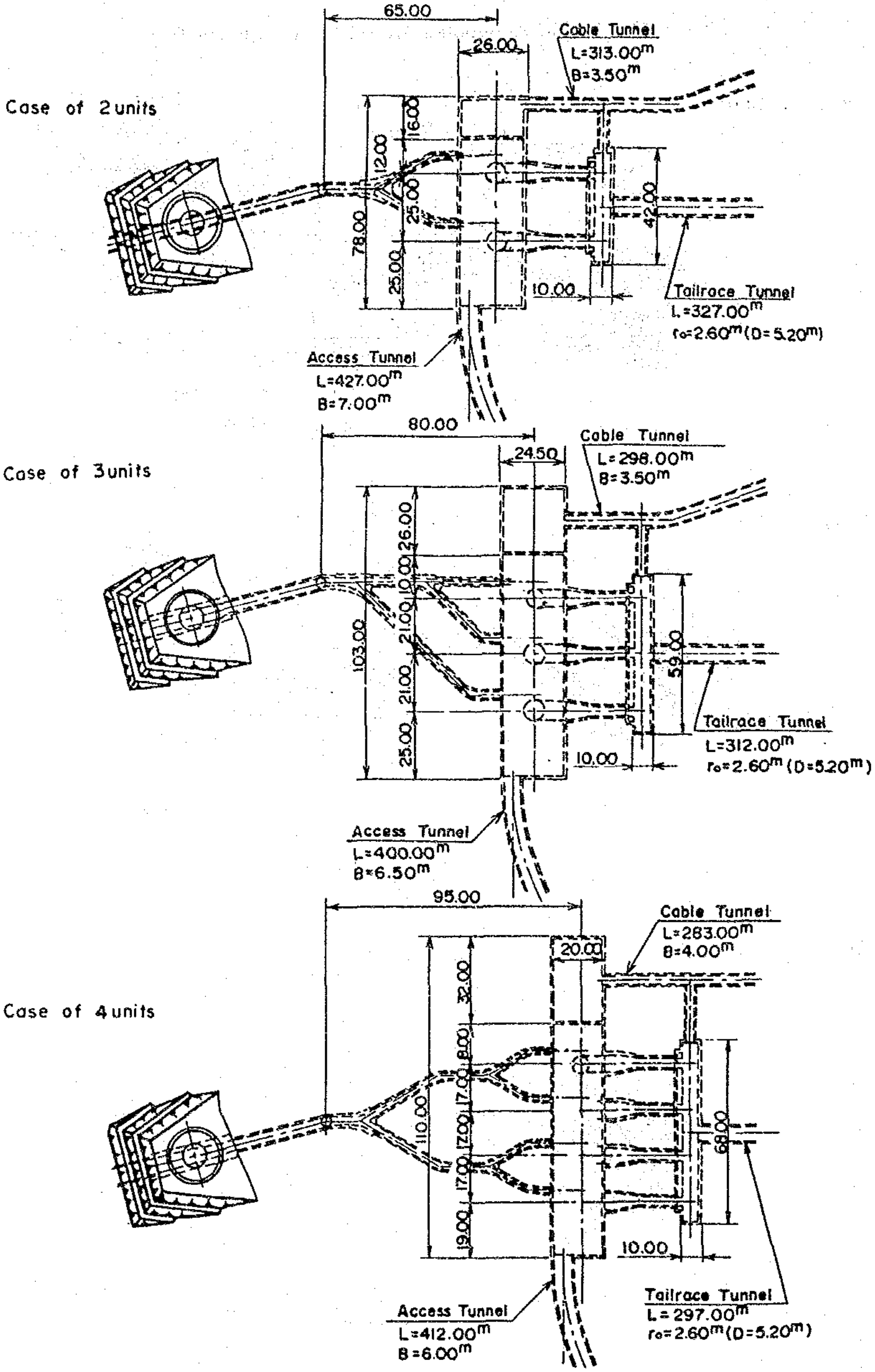

Fig. 7–22 Longitudinal Section of Each Turbine

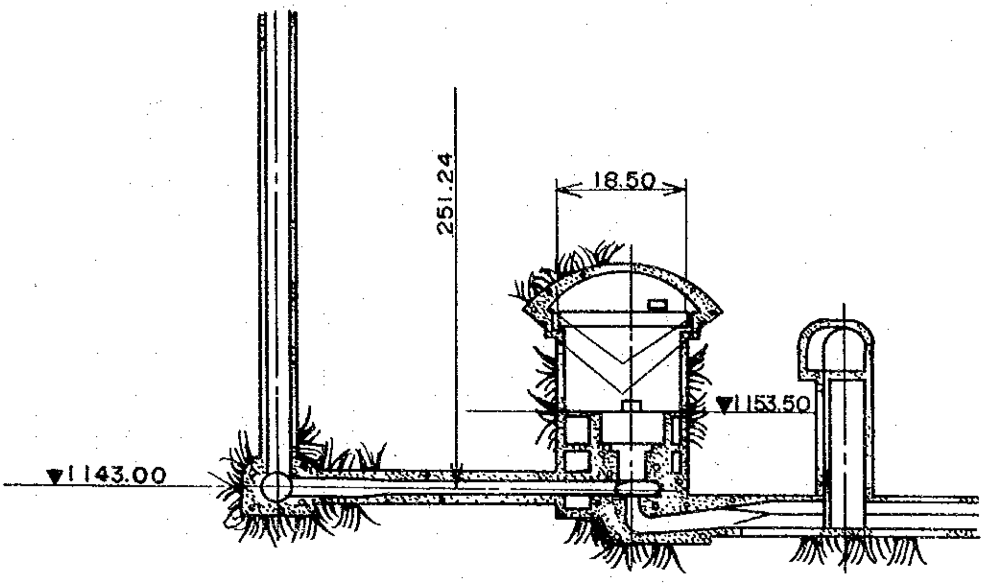

Francis turbine type (case of 2 units)

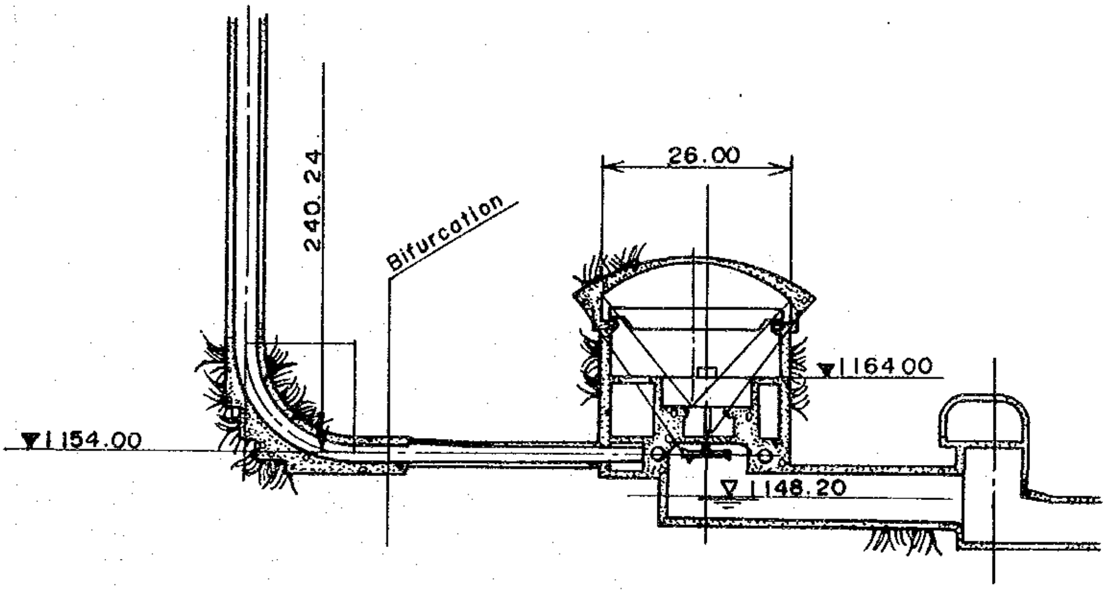

Pelton turbine type (case of 2 units)

Table 7–10 Comparison of Penstock Tunnel

	Frencis Type			Pelton Type		
	2 Units	3 Units	4 Units	2 Units	3 Units	4 Units
Length of penstock (m)	552.85	562.83	560.79	544.06	558.30	549.36
Front of bifurcation(m)	510.33	512.33	480.33	500.83	483.83	463.83
After of bifurcation(m)	42.52 x 2	42.20 44.70 50.50	44.38 x 2 36.08 x 4	43.23 x 2	57.50 65.77 74.47	51.65 x 2 33.88 x 4
Diameter of penstock						
Front of bifurcation (m)	4.50~3.00	4.50~3.00	4.50~3.00	4.50~3.00	4.50~3.00	4.50~3.00
After of bifurcation (m)	2.30~2.10	2.30~1.70	2.30~1.45	3.00~2.70	3.00~2.50	3.00~2.00
Loss head (m)	8.80	11.20	12.40	6.30	8.80	10.00
Excavation (open) (m³)	15 400	15 400	15 400	15 400	15 400	15 400
〃 (shaft)(m³)	1 200	1 200	1 200	1 000	1 000	1 000
〃 (tunnel)(m³)	4 100	5 400	6 600	4 700	5 800	6 600
Concrete (open) (m³)	5 460	5 460	5 460	5 460	5 460	5 460
〃 (filling)(m³)	2 730	3 950	5 090	2 980	3 810	4 560
Weight of steel penstock (ton)	1 110	1 180	1 260	1 150	1 210	1 260
Cost (x10³US $)	10 984	11 517	12 162	11 151	11 651	12 058

Table 7–11 Comparison of Powerhouse

	Frencis Type			Pelton Type		
	2 Units	3 Units	4 Units	2 Units	3 Units	4 Units
Width (W) (m)	28.00	25.50	23.50	35.50	34.00	29.50
Length (L) (m)	46.00	53.00	62.00	63.00	78.00	81.00
Height (H) (m)	44.50	43.50	42.50	38.00	37.50	36.00
Belong to building (control room and cable spreading room)	With power house	With power house	With power house	Without power house 12.00x20.00x20.00 (H) (B) (L)	Without power house 12.00x20.00x20.00 (H) (B) (L)	Without power house 12.00x20.00x20.00 (H) (B) (L)
℄ of turbine (m)	16.00	14.00	13.00	25.00	21.00	17.00
Tailrace water level (m)	1 145.30	1 145.30	1 145.30	1 152.50	1 152.50	1 152.50
Excavation (m^3)	169 300	190 800	217 700	167 000	187 200	193 000
Concrete (m^3)	33 650	38 850	46 790	41 050	50 960	54 270
Gate (ton)	54	66	68	41	46	48
Cost ($\times 10^3$ US $)						
Civil works	21 192	23 236	25 937	22 892	25 672	26 698
Electrical works	31 158	35 008	39 238	36 396	42 483	50 092
Total cost	52 350	58 244	65 175	59 288	68 155	76 790

Table 7—12 Comparison of Penstock Tunnel

	Frencis Type			Pelton Type		
	2 Units	3 Units	4 Units	2 Units	3 Units	4 Units
Length of penstock (m)	319.16	338.72	366.66	329.45	358.69	364.75
Front of bifurcation(m)	277.66	288.22	291.22	291.22	286.22	286.22
After of bifurcation(m)	41.50 x 2	42.20 44.70 50.50	44.38 x 2 31.06 x 4	38.23 x 2	55.50 63.77 72.47	48.65 x 2 29.88 x 4
Diameter of penstock						
Front of bifurcation (m)	3.80~3.00	3.80~3.00	3.80~3.00	3.80~3.00	3.80~3.00	3.80~3.00
After of bifurcation (m)	2.30~2.10	2.30~1.70	2.30~1.45	3.00~2.70	3.00~2.50	3.00~2.00
Loss head (m)	5.00	5.20	5.50	4.90	5.40	5.60
Excavation (shaft) (m³)	4 100	4 100	4 100	3 900	3 900	3 900
〃 (tunnel) (m³)	2 200	3 300	4 600	2 300	4 200	4 600
Concrete (shaft) (m³)	2 150	2 150	2 150	2 060	2 060	2 060
〃 (tunnel)(m³)	1 430	2 310	3 420	1 270	2 440	2 940
Weight of steel penstock (ton)	500	580	640	540	700	710
Cost (x10³US$)	7 005	7 696	8 351	7 131	8 369	8 556

Table 7–13–1 Comparison of Powerhouse

	Frencis Type			Pelton Type		
	2 Units	3 Units	4 Units	2 Units	3 Units	4 Units
1) Power house						
Width (W) (m)	18.50	16.00	14.50	26.00	24.50	20.00
Length (L) (m)	58.00	77.00	91.00	78.00	103.00	110.00
Height (H) (m)	39.00	38.00	36.50	38.00	37.00	35.50
Belong to building (control room and cable spreading room)	With switchyard 12.00x20.00x20.00	With switchyard 12.00x20.00x20.00	With switchyard 12.00x20.00x20.00	With switchyard 12.00x20.00x20.00	With switchyard 12.00x20.00x20.00	With switchyard 12.00x20.00x20.00
℄ of turbine (m)	16.00	14.00	13.00	25.00	21.00	17.00
Tailrace water level(m)	1 145.30	1 145.30	1 145.30	1 154.00	1 154.00	1 154.00
Excavation (m^3)	37 700	35 800	36 700	63 100	68 800	55 200
Concrete (m^3)	15 970	16 800	20 240	22 490	27 200	27 640
Cost $(\times 10^3\text{US}\$)$						
Civil works	8 476	9 538	10 463	13 858	15 681	14 484
Electrical works	31 713	36 021	40 654	36 783	43 375	51 429

Table 7—13—2 Comparison of Powerhouse

	Frencis Type			Pelton Type		
	2 Units	3 Units	4 Units	2 Units	3 Units	4 Units
2) Access tunnel						
Width (W) (m)	6.00	5.80	5.50	7.00	6.50	6.00
Length (L) (m)	431.40	412.75	388.40	427.40	400.00	412.00
Excavation (m^3)	18000	16 600	14 600	21900	18 700	17 300
Concrete (m^3)	2800	2 700	2 500	3 100	2 900	2 700
Cost of civil works ($x10^3$US$)	2 648	2 478	2 232	3 115	2 737	2 562
3) Cable tunnel						
Width (W) (m)	3.50	3.50	4.00	3.50	3.50	4.00
Length (L) (m)	327.81	312.80	282.80	313.00	298.00	283.00
Excavation (m^3)	5 400	5 200	5 500	5 200	4 900	5 500
Concrete (m^3)	1 930	1 840	1 820	1 840	1 750	1 820

Table 7–13–3 Comparison of Powerhouse

	Frencis Type			Pelton Type		
	2 Units	3 Units	4 Units	2 Units	3 Units	4 Units
Cost of civil works (x10^{3} US $)	1 073	1 033	1 055	1 033	974	1 055
3) Tailrace tunnel						
Diameter(D) (m)	3.70x3	3.10x3	2.60x3	5.20x1	5.20x1	5.20x1
Length (L) (m)	352.00	337.00	307.00	327.00	312.00	297.00
Excavation (m^3)	22 600	27 400	28 600	23 900	28 000	30 000
Concrete (m^3)	8 260	9 830	10 090	7 730	8 600	9 200
Gate (ton)	32	39	40	24	27	28
Cost of civil works (x10^{3} US $)	6 384	8 139	9 110	4 811	5 476	5 672
4) Out let						
Excavation (m^3)	800	1 200	1 700	1 400	1 400	1 400
Concrete (m^3)	550	820	1 100	630	630	630
Cost of civil works (x10^{3} US $)	139	206	282	184	184	184

Table 7–13–4 Comparison of Powerhouse

	Frencis Type			Pelton Type		
	2 Units	3 Units	4 Units	2 Units	3 Units	4 Units
5) Switchyard						
Width (W) (m)	60.00	60.00	60.00	60.00	60.00	60.00
Length(L) (m)	100.00	110.00	120.00	100.00	110.00	120.00
Excavation (m^3)	61 500	67 600	73800	61 500	67 600	73 800
Concrete (m^3)	1 610	1 780	1 960	1 610	1 780	1 960
Cost of civil works ($\times 10^3$ US $)	1 019	1 122	1 228	1 019	1 122	1 228
6) Access road						
Width (W) (m)	6.00	6.00	6.00	6.00	6.00	6.00
Length (L) (m)	350.00	350.00	350.00	350.00	350.00	350.00
Cost of civil works ($\times 10^3$ US $)	812	812	812	812	812	812
7) Total cost ($\times 10^3$ US $)						
Civil works	20 551	23 328	25 182	24 832	26 986	25 997
Electrical works	31 713	36 021	40 654	36 783	43 375	51 429
Total cost	52 264	59 349	65 836	61 615	70 361	77 426

Table 7–14 Comparison of Penstock Tunnel

	Frencis Type			Pelton Type		
	2 Units	3 Units	4 Units	2 Units	3 Units	4 Units
Length of penstock (m)	525.09	535.07	533.03	516.30	530.54	519.60
Front of bifurcation(m)	482.57	484.57	452.57	473.07	456.07	436.07
After of bifurcation(m)	42.52 x 2	42.20 44.70 50.50	44.38 x 2 36.08 x 4	43.23 x 2	57.50 65.77 74.47	51.65 x 2 31.88 x 4
Diameter of penstock						
Front of bifurcation (m)	4.50~3.00	4.50~3.00	4.50~3.00	4.50~3.00	4.50~3.00	4.50~3.00
After of bifurcation (m)	2.30~2.10	2.30~1.70	2.30~1.45	3.00~2.70	3.00~2.50	3.00~2.00
Loss head (m)	8.20	10.70	11.90	5.80	8.20	9.50
Excavation (open) (m³)	11 150	11 150	11 150	11 150	11 150	11 150
〃 (shaft) (m³)	2 550	2 550	2 550	2 110	2 110	2 110
〃 (tunnel) (m³)	3 890	4 880	6 090	4 340	5 390	6 130
Concrete (open) (m³)	4 800	4 800	4 800	4 800	4 800	4 800
〃 (filling) (m³)	3 020	3 330	5 470	3 030	3 950	4 830
Weight of steel penstock (ton)	1 200	1 250	1 290	1 150	1 200	1 240
Cost (x10³ US$)	11 391	11 687	12 369	11 150	11 612	11 993

Table 7–15–1 Comparison of Powerhouse

	Frencis Type			Pelton Type		
	2 Units	3 Units	4 Units	2 Units	3 Units	4 Units
1) Power house						
Width (W) (m)	28.00	25.50	23.50	35.50	34.00	29.50
Length (L) (m)	46.00	53.00	62.00	63.00	78.00	81.00
Height (H) (m)	44.50	43.50	42.50	38.00	37.50	36.00
Belong to building (control room and cable spreading room)	With power house	With power house	With power house	Without power house 12.00x20.00x20.00 (H) (B) (L)	Without power house 12.00x20.00x20.00 (H) (B) (L)	Without power house 12.00x20.00x20.00 (H) (B) (L)
℄ of turbine (m)	16.00	14.00	13.00	25.00	21.00	17.00
Tailrace water level (m)	1 133.30	1 133.30	1 133.30	1 140.50	1 140.50	1 140.50
Excavation (m³)	460 410	528 000	554 900	504 300	524 400	530 200
Concrete (m³)	49 860	55 060	63 000	57 260	67 170	70 480
Gate (ton)	32	39	40	24	27	28
Cost (x10³US $)						
Civil works	18 880	20 407	22 483	20 442	22 788	23 410
Electrical works	31 158	35 008	39 238	36 396	42 483	50 092

Table 7–15–2 Comparison of Powerhouse

	Frencis Type			Pelton Type		
	2 Units	3 Units	4 Units	2 Units	3 Units	4 Units
2) Access road						
Length (L) (m)	270.00	270.00	270.00	270.00	270.00	270.00
Width (W) (m)	6.00	6.00	6.00	6.00	6.00	6.00
Cost of civil works ($\times 10^3$ US $)	562	562	562	562	562	562
Total cost ($\times 10^3$ US $)	50 600	55 977	62 283	57 400	65 833	74 064

Table 7–16 Comparison of Penstock Tunnel

	Frencis Type			Pelton Type		
	2 Units	3 Units	4 Units	2 Units	3 Units	4 Units
Length of penstock (m)	442.26	461.82	489.76	452.55	481.79	487.85
Front of bifurcation(m)	400.76	411.32	414.32	414.32	409.32	409.32
After of bifurcation(m)	41.50 x 2	42.20 44.70 50.50	44.38 x2 31.06 x4	38.23 x 2	55.50 63.77 72.47	48.65 x 2 29.88 x 4
Diameter of penstock						
Front of bifurcation (m)	3.80~3.00	3.80~3.00	3.80~3.00	3.80~3.00	3.80~3.00	3.80~3.00
After of bifurcation (m)	2.30~2.10	2.30~1.70	2.30~1.45	3.00~2.70	3.00~2.50	3.00~2.00
Loss head (m)	6.20	6.40	6.70	6.10	6.50	6.80
Excavation (open) (m³)	5 500	5 500	5 500	5 500	5 500	5 500
〃 (shaft) (m³)	3 900	3 900	3 900	3 700	3 700	3 700
〃 (tunnel)(m³)	4 100	5 000	6 200	4 000	5 900	6 300
Concrete (open) (m³)	2 200	2 200	2 200	2 200	2 200	2 200
〃 (shaft) (m³)	2 080	2 080	2 080	1 990	1 990	1 990
〃 (tunnel)(m³)	2 390	3 170	4 250	2 100	3 320	3 820
Weight of steel penstock (ton)	700	780	840	740	900	910
Cost (x10³US$)	8 918	9 543	10 184	8 988	10 221	10 408

Table 7–17–1 Comparison of Powerhouse

	Frencis Type			Pelton Type		
	2 Units	3 Units	4 Units	2 Units	3 Units	4 Units
1) Power house						
Width (W) (m)	18.50	16.00	14.50	26.00	24.50	20.00
Length (L) (m)	58.00	77.00	91.00	78.00	103.00	110.00
Height (H) (m)	39.00	38.00	36.50	38.00	37.00	35.50
Belong to building (control room and cable spreading room)	With switchyard 12.00x20.00x20.00	With switchyard 12.00x20.00x20.00	With switchyard 12.00x20.00x20.00	With switchyard 12.00x20.00x20.00	With switchyard 12.00x20.00x20.00	With switchyard 12.00x20.00x20.00
℄ of turbine (m)	16.00	14.00	13.00	25.00	21.00	17.00
Tailrace water level(m)	1 133.30	1 133.30	1 133.30	1 141.50	1 141.50	1 141.50
Excavation (m^3)	37 700	35 800	36 700	63 100	68 800	55 200
Concrete (m^3)	15 970	16 800	20 240	22 490	27 200	27 640
Cost (x10^{3}US \$)						
Civil works	8 476	9 538	10 463	13 858	15 681	14 484
Electrical works	31 713	36 021	40 654	36 783	43 375	51 429

Table 7–17–2 Comparison of Powerhouse

	Frencis Type			Pelton Type		
	2 Units	3 Units	4 Units	2 Units	3 Units	4 Units
2) Access tunnel						
Width (W) (m)	6.00	5.80	5.50	7.00	6.50	6.00
Length (L) (m)	457.10	438.45	414.10	453.10	425.70	437.70
Excavation (m^3)	19 100	17 500	15 500	23 200	19 800	18 300
Concrete (m^3)	2 900	2 800	2 600	3 200	3 000	2 800
Cost of civil works ($\times 10^3$ US $)	2 689	2 508	2 262	3 157	2 788	2 593
3) Cable tunnel						
Width (W) (m)	3.50	3.50	4.00	3.50	3.50	4.00
Length (L) (m)	384.60	369.59	339.59	369.79	354.79	339.79
Excavation (m^3)	6 400	6 100	6 600	6 100	5 900	6 600
Concrete (m^3)	2 260	2 170	2 190	2 170	2 090	2 190

Table 7–17–3 Comparison of Powerhouse

	Frencis Type			Pelton Type		
	2 Units	3 Units	4 Units	2 Units	3 Units	4 Units
Cost of civil works ($\times 10^3$ US $)	1 265	1 206	1 256	1 206	1 168	1 256
3) Tailrace tunnel						
Diameter (D) (m)	3.70x2	3.10x3	2.60x4	5.20x1	5.20x1	5.20x1
Length (L) (m)	190.00	175.00	145.00	165.00	150.00	135.00
Excavation (m^3)	16 400	20 600	21 900	17 900	22 100	24 000
Concrete (m^3)	5 660	6 870	7 050	5 590	6 450	7 060
Gate (ton)	32	39	40	24	27	28
Cost of civil works ($\times 10^3$ US $)	4 290	5 513	5 952	3 490	4 155	4 543
4) Out let						
Excavation (m^3)	800	1 200	1 700	1 400	1 400	1 400
Concrete (m^3)	550	820	1 100	630	630	630
Cost of civil works ($\times 10^3$ US $)	139	206	282	184	184	184

Table 7—17—4 Comparison of Powerhouse

	Frencis Type			Pelton Type		
	2 Units	3 Units	4 Units	2 Units	3 Units	4 Units
5)Switchyard						
Width (W) (m)	60.00	60.00	60.00	60.00	60.00	60.00
Length(L) (m)	100.00	110.00	120.00	100.00	110.00	120.00
Excavation (m³)	61 500	67 600	73 800	61 500	67 600	73 800
Concrete (m³)	1 610	1 780	1 960	1 610	1 780	1 960
Cost of civil works (x10³ US $)	1 019	1 122	1 228	1 019	1 122	1 228
6)Access road						
Width (W) (m)	6.00	6.00	6.00	6.00	6.00	6.00
Length (L) (m)	150.00	150.00	150.00	150.00	150.00	150.00
Cost of civil works (x10³US $)	312	312	312	312	312	312
7) Total cost (x10³US $)						
Civil works	18 190	20 405	21 755	23 226	25 410	24 600
Electrical works	31 713	36 021	40 654	36 783	43 375	51 429
Total cost	49 903	56 426	62 405	60 009	68 785	76 029